AGU PUBLICATIONS

JGR

Journal of Geophysical Research: Oceans

RESEARCH ARTICLE

10.1002/2014JC010022

Intrusion of Rhone River diluted water into the Bay of Marseille: Generation processes and impacts on ecosystem functioning

Marion Fraysse[1,2], Ivane Pairaud[1], Oliver N. Ross[2], Vincent M. Faure[2], and Christel Pinazo[2]

[1]Institut Français de Recherche pour l'Exploitation de la Mer, Laboratoire Environnement Ressources Provence Azur Corse, La Seyne sur Mer, France, [2]Aix Marseille Université, CNRS, Université de Toulon, IRD, MIO UM 110, 13288, Marseille, France

Key Points:
- Rhone River intrusions into the Bay of Marseille were modeled
- Rhone River intrusions are characterized based on their generation mechanisms
- Rhone intrusions are of high ecological significance for the Bay of Marseille

Correspondence to:
M. Fraysse,
marion.fraysse@univ-amu.fr; C. Pinazo,
christel.pinazo@univ-amu.fr

Citation:
Fraysse, M., I. Pairaud, O. N. Ross, V. M. Faure, and C. Pinazo (2014), Intrusion of Rhone River diluted water into the Bay of Marseille: Generation processes and impacts on ecosystem functioning, *J. Geophys. Res. Oceans*, *119*, 6535–6556, doi:10.1002/2014JC010022.

Received 4 APR 2014
Accepted 2 SEP 2014
Accepted article online 5 SEP 2014
Published online 1 OCT 2014

Abstract The Rhone River provides the largest inputs of terrestrial freshwater and nutrients into the Mediterranean Sea. The Rhone River diluted water intrusions into the Bay of Marseille were investigated, examining their physical generation processes and associated biogeochemical impact by using in situ observations, remote sensing data, and a three-dimensional physical/biogeochemical coupled model. During our study period from 2007 to 2011, Rhone River intrusions occurred on average 7.6 times per year and affected more frequently the northern part of the bay. A classification of intrusion events in three categories is proposed (short lived, big, and small) as a function of their duration and spatial extent. The intrusions appeared to be driven by: (i) wind forcing, (ii) the presence of a mesoscale eddy, (iii) the Rhone River discharge volume, and (iv) the variation in thermocline depth. Typically, a combination of these favorable factors was necessary to induce an intrusion. An intrusion strongly impacts the biogeochemical functioning of the Bay of Marseille by bringing large quantities of nutrients into the bay. Mass balances were computed allowing us to quantify this impact on the Bay of Marseille. The results show that the ecological impact depends very much on the type of intrusion, with big intrusions having the highest impact.

1. Introduction

Coastal zone ecosystems are often subject to a wide range of anthropogenic pressures rendering them vulnerable and prone to overexploitation. *Craig and Ruhl* [2010] argue that the present use of coasts is unsustainable under any definition, and that an increased protection of coastal ecosystems—paying particular attention to ecosystem functioning and the interplay between physics, chemistry, and biology—is critical to achieve sustainability. To assist local managers and decision makers in this task, it is imperative to collect as much data and information as possible. This will not only improve our understanding of the structure and functioning of the ecosystem as a whole [*Elliott*, 2011] but also help with quantifying both the human impact and the value of ecosystem services to society and local stakeholders. To this end, ecosystem modeling approaches are useful tools to improve our understanding of the complex coastal environments because they can help to identify the dominant forcings, distinguish between natural and anthropogenic components, and quantify their respective impacts on the ecosystem.

Marseille is the second largest city in France (Figure 1) with a population of over 1 million. Human activities strongly impact the marine environment of the Bay of Marseille, especially during flood events [*Oursel et al.*, 2014], when high concentrations of nutrients and chemicals are released by the waste water treatment plant into the sea. However, even during these extreme flood events the associated water flow is much smaller than the average Rhone River input of chemicals and nutrients into the Gulf of Lions. In a previous study, the coupled 3-D hydrodynamic ecosystem model (MARS3D-RHOMA/ECO3M-MASSILIA-P) was developed in order to better understand the biogeochemical functioning of the coastal pelagic ecosystem of the Marseille area. In a first study, *Fraysse et al.* [2013] concluded that the ecosystem functioning of the Bay of Marseille (BoM) is complex and strongly affected by the hydrodynamics and terrestrial inputs. The Rhone River does not flow directly into the Bay of Marseille but is located about 35 km to the West. It represents the largest input of freshwater into the Mediterranean Sea with a mean inflow of around 1700 $m^3\ s^{-1}$ [*Pont et al.*, 2002], which divide into two unequal distributaries: the "Grand Rhone" (90%) and the "Petit Rhone" (10%) [*Ibanez et al.*, 1997; *Pont et al.*, 2002]. The Rhone River receives many anthropogenic inputs along its course to the Mediterranean, including diverse industrial discharges, outflows from sewage plants, and

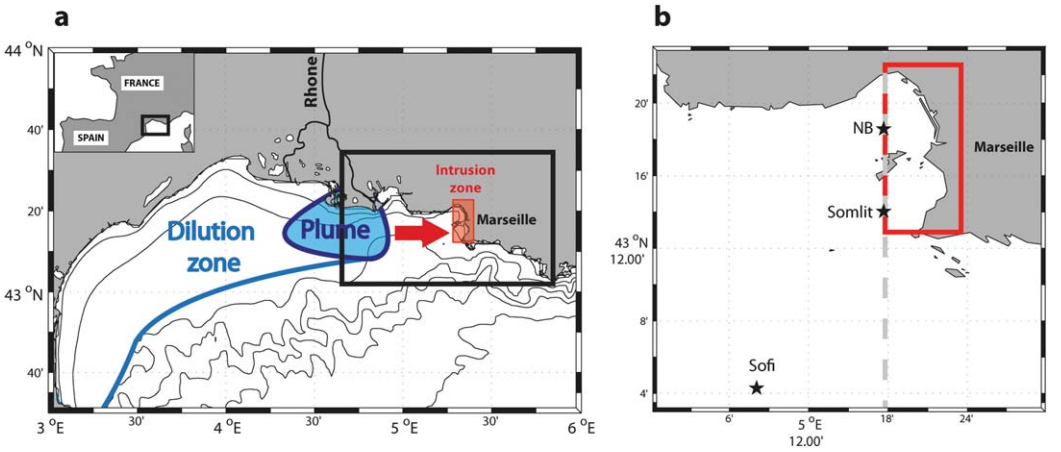

Figure 1. (a) Bathymetric map of the Gulf of Lions with the Rhone River plume, the dilution zone (in blue), the model domain (in black), and the zone defining a Rhone River intrusion in the Bay of Marseille (in red); (b) zoom on the Bay of Marseille. The red rectangle shows the boundaries we defined for the Bay of Marseille and the area for which we calculate mass budgets during intrusion events. Also visible are the Somlit station (43°14.30′N; 5°17.30′E), the Sofi station (5°7.8′E; 43°4.2′N), and the Northern Bay station (NB) (43°18.66′N; 5°17.30′ E).

runoffs from agricultural regions resulting in large quantities of nitrogen, phosphorus, and carbon stored and transported as organic and inorganic matter [*Pujo-Pay et al*., 2006].

It has been estimated that the nutrient input from the Rhone River could support between 23% and 69% of the average primary production (PP) in the Gulf of Lions (GoL) [*Ludwig et al*., 2009], which is one of the most productive areas of the Mediterranean Sea [*Durrieu de Madron et al*., 2011]. The biogeochemical characteristics of the Rhone River plume in the vicinity of the river mouth have been extensively investigated [*Naudin et al*., 2001; *Pujo-Pay et al*., 2006]. Within the plume, the effects of temperature, light conditions, and suspended matter on biological activity seem relatively minor compared to those induced by differences in salinity and nutrient availability [*Naudin et al*., 2001]. The initial mineral N:P ratio in the Rhone River plume averages around 65:1 to 70:1 which further exacerbates the well-known phosphate deficiency in this part of the Mediterranean [*Pujo-Pay et al*., 2006]. Diluted mesoscale structures of lower-salinity water (LSW) can become detached from the Rhone River plume, and be transferred to the continental shelf and toward the open Mediterranean Sea. The biogeochemical processes in these LSW structures and their temporal evolution have recently been investigated as they constitute natural "macrocosms" in which biological processes modify dissolved and particulate material during the offshore transfer [*Diaz et al*., 2008; *Auger et al*., 2011].

The Rhone River plume dynamics have been studied both from observations [*Broche et al*., 1998; *Forget and Ouillon*, 1998; *Gatti et al*., 2006] and using numerical models [*Estournel et al*., 2001; *Arnoux-Chiavassa et al*., 2003; *Reffray et al*., 2004]. While the Rhone River plume is typically deflected westward (clockwise) due to the Coriolis acceleration, these previous studies showed that both the horizontal and vertical extent of the plume depend on the atmospheric conditions, the Rhone River discharge volume, and the ambient circulation. The GoL is dominated by two distinct wind regimes that induce two types of plume dynamics: under north-northwesterly winds (e.g., Mistral), the plume extends offshore toward the southwest, while southeasterlies typically push and contain the plume near the coast, to the west of the river mouth [*Demarcq and Wald*, 1984].

More recently, a less common orientation of the plume has been observed where the plume extended approximately 40 km eastward from the Rhone River mouth and several kilometers offshore from the Bay of Marseille (BoM) to the SOFI sampling site (5.131°E, 43.071°N; Figure 1) [*Gatti et al*., 2006]. In their study, *Gatti et al*. [2006] used a salinity threshold of 37.8 to identify the presence of diluted water from the Rhone River plume. In another study (SORCOM cruises), *Younes et al*. [2003] used a slightly lower threshold of 37.3 to conclude that a freshwater influence could be detected in the BoM only during 5% of the time they were sampling. More recently, both modeling studies [*Pairaud et al*., 2011; *Schaeffer et al*., 2011] and observations [*Gatti et al*., 2006; *Para et al*., 2010] have suggested that water from the Rhone River may be present in the BoM more frequently than previously thought and that it may have a measurable impact on the local biogeochemistry.

Gatti et al. [2006] formulated three hypotheses which could explain this eastward extent of the region of freshwater influence (ROFI). Their first hypothesis was based on the occurrence of a storm event in combination with easterly winds and high Rhone River discharges. The second hypothesis focused on the Northern Current (NC) mesoscale activity, which is particularly strong in winter. As the NC is a strong and persistent slope current which meanders along the GoL shelf break, an anticyclonic eddy could detach from the NC near the SOFI site, the northern part of which could produce the observed eastward current at the SOFI station, thereby advecting Rhone River waters eastward. Finally, they suggested a third hypothesis that takes into account more complex generation processes such as the interplay between the wind-driven local circulation and the bathymetry. The existence of a nearshore eastward flow could thus be one of the GoL's particular circulation features that develop on the shelf and may be linked to anticyclonic eddies that become trapped at topographic irregularities due to the interaction between barotropic shelf waves and the NC flowing along the shelf break. Such anticyclonic eddies were reported by *Allou et al*. [2010] and also by *Schaeffer et al*. [2011] who named it the Marseille Eddy (ME).

The 3-D coupled hydrodynamic-biogeochemical model (MARS3D-RHOMA/ECO3M-MASSILIA-P) was developed to improve our understanding of the biogeochemical processes in the coastal pelagic ecosystem off the coast of Marseille. *Fraysse et al*. [2013] simulated the period from 2007 to 2011 and found that the model was capable to reproduce most of the physical and biogeochemical processes of the coastal area. They concluded that the ecosystem functioning of the BoM was complex and predominantly driven by the hydrodynamics and terrestrial inputs. Intrusion events of Rhone River diluted water into the BoM are therefore an important physical/biogeochemical driver which could strongly impact the local ecosystem.

Typically, the Rhone River plume is displaced westward and does not reach the BoM. Only during a few occasions per year, this pattern is broken and the plume is displaced eastward, entering the BoM. In this study, we call "Rhone River intrusion" (RRI) the advection of low-salinity ($<$37.8) diluted water from the Rhone River to regions east of 5°17.30′E. The purpose of this study is thus twofold: (i) we examine the physical conditions under which such intrusions of Rhone River water occur in the BoM, and (ii) we quantify the biogeochemical impact of these nutrient-rich plume waters on the otherwise oligotrophic BoM. The pelagic ecosystem of the BoM is mainly oligotrophic and the effects of RRI events in the BoM have not yet been investigated. This paper aims to improve our understanding of these events including their impacts on the biogeochemistry and ecosystem functioning in the BoM. We first characterize the RRIs in terms of frequency, seasonal occurrence, and spatial extension, and then examine their generation processes, formulating a hypothesis on how to identify different kinds of intrusions. Finally, we examine the impacts in the BoM of different intrusion events on the biogeochemical functioning of the lower trophic levels.

2. Materials and Methods

2.1. The 3-D Coupled Physical/Biogeochemical Model

2.1.1. Model Description

The hydrodynamic model MARS3D (Model At Regional Scale 3-D) [*Lazure and Dumas*, 2008] in its RHOMA version [*Pairaud et al*., 2011] was coupled to the biogeochemical modeling tool ECO3M (Ecological Mechanistic and Modular Model) [*Baklouti et al*., 2006; *Faure et al*., 2006, 2010] in its MASSILIA-P version (i.e., with added phosphorous cycle) adapted to the Marseille coastal area [*Fraysse et al*., 2013].

The horizontal model resolution was 400 m, leading to a grid of 252 $\times$ 120 horizontal cells with 30 vertical sigma levels [*Fraysse et al*., 2013]. The hydrodynamic model and the biogeochemical model were coupled online. The biogeochemical model operates on a time step of 20 min while the physical advection-diffusion of biogeochemical tracers occurs with a 30 s time step.

The biogeochemical model ECO3M-MASSILIA-P (17 state variables) implements mechanistic formulations to describe the carbon, nitrogen, and phosphorus cycles in five compartments: (i) phytoplankton, (ii) bacteria, (iii) detrital particulate organic matter, (iv) labile dissolved organic matter, and (v) dissolved inorganic matter including ammonium, nitrate, and oxygen. Chlorophyll-*a* is a diagnostic variable related to the variable phytoplankton ratios. A more detailed description of the model can be found in *Fraysse et al*. [2013].

The ability of the hydrodynamic model to successfully reproduce intrusions of diluted Rhone River water was demonstrated by *Pairaud et al*. [2011] and *Fraysse et al*. [2013] who showed that the seasonal signal in both nutrients and chlorophyll-*a* was well represented.

2.1.2. Modeling Experiments

Realistic simulations were performed for the years 2007–2011 and the model domain is shown in Figure 1. The model takes into account the biogeochemical input from various sources (atmospheric deposition, riverine, etc.) as well as physical forcing (general circulation at the boundaries, wind, rain and heat flux from the atmosphere). In this microtidal area, hydrodynamic and biogeochemical forcing was provided by a coupled model with a coarse resolution (1.2 km). A detailed description of both the physical and biogeochemical forcing are available in *Pairaud et al*. [2011] and *Fraysse et al*. [2013], respectively.

We conducted a range of different modeling experiments in order to investigate specific processes. A first experiment was set up in order to explore the role that the size of the Rhone River discharge plays in the generation of the observed eastward intrusions of the plume. Two simulations were performed for the years 2007–2011: one with a realistic and seasonally varying Rhone River discharge ranging from 200 to 6680 m^3 s^{-1} (run REF) and another with a constant and relatively low Rhone discharge equal to 600 m^3 s^{-1} (run R600).

A second experiment was set up in order to evaluate the impact of Rhone River inputs on the ecology of the Bay of Marseille during an intrusion event. To this end, a simulation was performed where the Rhone River did not contain any biogeochemical substances (run NoRhone) to be compared to the control (run REF, see above). The REF and NoRhone simulations were performed with identical Rhone River freshwater discharge volumes in order to leave the hydrodynamics unaffected. In order to eliminate the influence of any Rhone River substances still in the system, we waited for 1 month after turning off the biogeochemical input before beginning the analysis. Previous studies have shown that the residence time of riverine inputs in this coastal area is typically lower than 1 month and for most processes terrogenic nutrients have been exhausted after a time scale of less than 1 week [*Jany et al*., 2012].

2.2. Postprocessing Methods Applied on Model Results

Due to the increasing quantity and the specific type of data obtained from large 3-D physical/biogeochemical models, there is a need for effective feature extraction methods. In this paper, we used Self-Organizing Maps (Appendix A) and also different indices plus an eddy detection algorithm and mass budget analyses.

2.2.1. Indices

2.2.1.1. River Plume Index

We used the equivalent depth of freshwater δ_{fw} [*Choi and Wilkin*, 2007; *Huret et al*., 2012] as an index to characterize the river plume:

$$\delta_{fw} = \int_{-H}^{Xe} \frac{S_{ref} - S_z}{S_{ref}} dz \tag{1}$$

S_{ref} is a reference salinity taken as the maximum value found in the model results at each time step, S_z is the salinity at the depth z, H the maximum depth of the water column in meters that is taken into account, and Xe is the surface elevation in meters.

H was set to 50 m in order to be able to account for deep intrusion events like the salinity decrease down to 40 m which was observed at the SOFI station in December 2003 [*Gatti et al*., 2006], while excluding deep processes that occur at the seabed such as the influx of deep Mediterranean water from the canyons.

2.2.1.2. Thermocline Depth

The thermocline depth (Z_{th}) was estimated from the following expression:

$$\text{if} \quad T_{zo} - T_{zb} \geq 0.5^{\circ}C, \quad Z_{th} = \left. Z \right|_{\max\left(\frac{\partial T}{\partial z}\right)} \text{ with } Z_{th} \in [2, H] \tag{2}$$

It is based on three criteria: (i) Z_{th} was only computed if the difference between the surface temperature (T_{zo}) and the bottom temperature (T_{zb}) was greater than 0.5°C; (ii) Z_{th} has to coincide with the depth of the maximum vertical gradient [*Huret et al*., 2012]; and (iii) Z_{th} must be located below 2 m to avoid detecting skin effects.

2.2.2. Eddy Detection

We used a vector geometry-based eddy detection algorithm [*Nencioli et al*., 2010] to identify and track eddies in the model output. The Eddy tracking package V2.1 was downloaded from http://www.com.univ-mrs.fr/~nencioli/research.php?type=submeso. Following the recommendation by *Nencioli et al*. [2010], we

Table 1. Mass Budgets Calculated in the Bay of Marseille Box for Each Biogeochemical Substance (*BS*)[a]

Symbol	Definitions
$B^X(BS,t)$	Evolution of the stock from source *X* of a biogeochemical substance (*BS*) within the Bay of Marseille relative to the initial stock at time t_0
$X = TOT$	Evolution of the total stock
$X = OB$	Contribution by in/outflow across the open boundaries
$X = BIO$	Contribution by biogeochemical processes (source or sink), such as local production
$X = ATM$	Inputs due to atmospheric deposition
$X = UR$	Inputs by urban rivers which flow directly into the Bay of Marseille box (this excludes the Rhone River)
$B^{TOT}_{RHONE}(BS,t)$	Evolution of the total stock due to the Rhone River
$B^{BIO}_{RHONE}(BS,t)$	Changes due to biogeochemical processes caused by biogeochemical substances inputs from the Rhone River (e.g., enhanced local production)
$B^{OB}_{RHONE}(BS,t)$	Contribution of the Rhone River biogeochemical substances to in/outflow across the open boundaries

[a]Examples for biogeochemical substances are the different nutrients or chlorophyll-*a*.

started by visually comparing the algorithm results against manual detection for some selected time steps. It allowed us to fix the two parameters used for eddy center detection depending on selected constrains to $a = 4$, $b = 2$ (for a detailed explanation of this method and the meaning of a and b, see *Nencioli et al*. [2010, p. 567]). The number of grid points which defines the initial area to compute the eddy dimensions was set to $rad = 20$.

2.2.3. Mass Budgets

We evaluated the mass budget (variation in total mass) $B^{TOT}(BS,t)$ for each biogeochemical substance (BS) in the Bay of Marseille (boxed area in Figure 1), distinguishing between gains/losses due to various sources/sinks: atmospheric ($B^{ATM}(BS,t)$, source only), urban rivers ($B^{UR}(BS,t)$, source only), biogeochemical process ($B^{BIO}(BS,t)$, source or sink), and exchanges across the open boundaries of the box ($B^{OB}(t)$, source or sink) (equation (3), Table 1, Appendix B). This yields the total mass budget for the Bay of Marseille:

$$B^{TOT}(BS,t) = B^{OB}(BS,t) + B^{BIO}(BS,t) + B^{ATM}(BS,t) + B^{UR}(BS,t) \tag{3}$$

It should be noted that the Rhone River mouth is not located in the Bay of Marseille but several kilometers to the West. Its contribution is therefore not contained in $B^{UR}(BS,t)$ but is included in $B^{OB}(BS,t)$.

We subtracted the budgets obtained from the "NoRhone" simulation ($B_{NoRhone}$) from the budgets of the "REF" simulation (B_{REF}) in order to obtain the contribution from the Rhone $B^{TOT}_{RHONE}(BS,t)$.

$$\begin{aligned} B^{TOT}_{RHONE}(BS,t) &= B^{TOT}_{REF}(BS,t) - B^{TOT}_{NoRhone}(BS,t) \\ &\overset{Eq(3)}{=} \left[B^{OB}_{REF}(BS,t) - B^{OB}_{NoRhone}(BS,t)\right] + \left[B^{BIO}_{REF}(BS,t) - B^{BIO}_{NoRhone}(BS,t)\right] \\ &= B^{OB}_{RHONE}(BS,t) + B^{BIO}_{RHONE}(BS,t) \end{aligned} \tag{4}$$

$B^{ATM}(BS,t)$ and $B^{UR}(BS,t)$ are identical in the REF and NoRhone scenarios and do therefore cancel out in the subtraction (equation (4)) which only leaves us with the "OB" and "BIO" components.

2.3. Observational Data Sets

We used a long time series of hydrobiogeochemical data collected twice monthly at the SOMLIT station (cf. Figure 1) to compare with model results. High vertical resolution profiles of temperature, salinity, and oxygen were obtained between 0 and 55 m using a conductivity-temperature-depth-oxygen profiler (CTDO, Seabird 19+). The concentrations of dissolved oxygen, NH_4, NO_3, PO_4, particulate organic carbon (POC), particulate organic nitrogen (PON), and chlorophyll-*a* were analyzed at three depths: at 1 m, at the depth containing the chlorophyll-*a* maximum, and at 55 m. The data were provided by the SOMLIT network (Service d'Observation en Milieu Littoral, http://somlit.epoc.u-bordeaux1.fr).

Daily averaged discharge data for 2007–2011 at the Beaucaire station were obtained from the "Compagnie Nationale du Rhone." The "Grand Rhone" discharge was taken as 90% of the total Rhone River discharge.

Remote sensing data (ocean color) from the MODIS AQUA and the MERIS ENVISAT sensors were processed using the OC5 algorithm [*Gohin et al*., 2002, 2005] to estimate chlorophyll-*a* concentrations. The MODIS and MERIS ocean color maps have a spatial resolution of approximately 1 km, which is coarser than the spatial

Table 2. Inventory of Rhone River Intrusions and the Frequency of Their Occurrence for Different Months of the Year During the 2007–2011 Period[a]

	Number of Intrusion Events						
	2007	2008	2009	2010	2011	2007–2011	Total Share (%)
Jan	1	0	1	0	0	2	5
Feb	1	0	0	0	0	1	3
Mar	2	0	0	0	0	2	5
Apr	0	0	0	1	0	1	3
May	0	1	1	0	1	3	8
Jun	3	2	2	1	0	8	21
Jul	3	2	2	1	0	8	21
Aug	0	1	0	1	0	2	5
Sep	1	0	1	0	1	3	8
Oct	0	1	1	2	0	4	11
Nov	0	0	1	0	0	1	3
Dec	0	1	0	1	1	3	8
Total	11	8	9	7	3	38	100

[a]The last column contains the total percent share for each month.

resolution of our model (400 m). The quality of the remote sensing data was already evaluated by *Fraysse et al*. [2013].

2.4. Rhone River Intrusion Event Inventory

In order to count the number of RRIs in the Bay of Marseille, it was necessary to establish a clear definition of this event. In this study, a RRI is said to occur whenever water with a salinity lower than 37.8 is advected eastward of 5°17.30′E (the longitude of the SOMLIT station). Intrusion was also detectable on remote sensing data of surface chlorophyll-*a* as Rhone diluted waters are often associated with elevated concentrations in chlorophyll-*a* [*Para et al*., 2010, Figure 2; *Pairaud et al*., 2011, Figure 10]. As an additional safeguard, RRIs detected from the model results were only counted if they could also be seen in the in situ salinity data at the SOMLIT station or in remote sensing data of surface chlorophyll-*a*.

3. Results

3.1. Characterization of Rhone River Diluted Water Intrusion in the Bay of Marseille

3.1.1. Rhone River Intrusion Inventory

The inventory of RRIs (Table 2) shows a total of 38 intrusion events during the years 2007–2011, which corresponds to an average of 7.6 intrusions per year lasting a total of 17 days. Intrusion events seem to be particularly common during the months of June and July, when RRIs are detected approximately 4 times more often compared to the rest of the year. Another slightly above-average occurrence is observed during the month of October. These results were confirmed by the model analysis with Self-Organizing Maps (Appendix A). Based on their spatial coverage and duration, we divided the intrusion events into three different categories:

1. The first category—called "big"—contains RRIs that had a **large** spatial coverage and a **long** duration.
2. The second category—called "short lived"—contains RRIs that had a **large** spatial coverage and a **short** duration.
3. The third category—called "small"—contains RRIs that had a **small** spatial coverage and a **short** duration.

In order to characterize these different types of intrusions in more detail, we focus on two contrasting examples: (1) an RRI in June 2008, which falls into the "big" category and which was already studied by *Pairaud et al*. [2011]; (2) an RRI that occurred in May 2011 to represent the "small" category. The June 2008 intrusion began on 16 June and lasted 10 days, whereas the May 2011 intrusion began on 19 May and lasted only 3 days.

3.1.2. Characterizing the Intrusions Events

If we compare the modeled surface salinity maps during these intrusion events (Figures 2a and 2b), we find lower absolute salinities in the BoM during the big intrusion in June 2008 compared to the small event in May 2011, with values of 35 and 37.2, respectively.

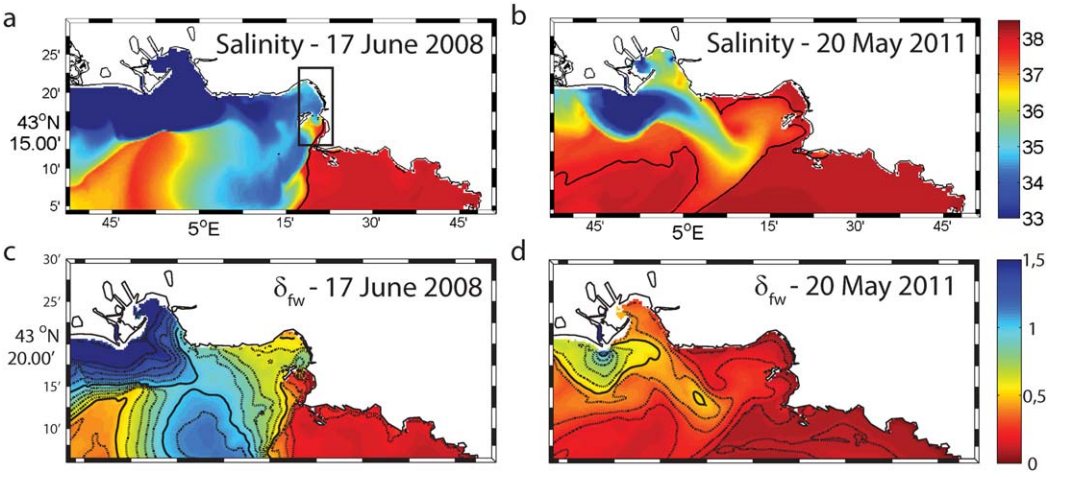

Figure 2. Modeled surface salinities on (a) 17 June 2008 and (b) 20 May 2011. Modeled equivalent depth of freshwater (in m) on (c) 17 June 2008 and (d) 20 May 2011.

In order to characterize the horizontal and vertical extent of the Rhone River diluted water in terms of salinity, we computed the equivalent depth of freshwater δ_{fw} (Figures 2c and 2d). The horizontal extent of the area where the plume had a $\delta_{fw} > 0.5$ m was very different in the two intrusion events. In May 2011, it was limited to a small area near the mouth, due to low discharge during the week preceding the event (7 day mean of 560 $m^3\ s^{-1}$). In June 2008, this area was considerably larger due to higher discharge volumes (mean of 2395 $m^3\ s^{-1}$) during the preceding week.

The intrusion affected a much smaller area in the Bay of Marseille during the event in May 2011 compared to the event in June 2008. In the Bay of Marseille itself, $\delta_{fw} < 0.2$ m during the 2011 event while in 2008 the entire northern bay and most of the southern bay had 0.4 m $< \delta_{fw} <$ 0.8 m.

3.2. Generation Mechanisms for Rhone River Intrusions

In order to improve our understanding of the physical processes which lead to Rhone River intrusions in the Bay of Marseille, we evaluated the relative importance of the main environmental forcings which could be involved in the generation process.

3.2.1. Rhone River Discharge

Commensurate with previous studies [*Gatti et al*., 2006; *Pairaud et al*., 2011], we expected high Rhone River discharge volumes to be crucial to produce an intrusion event in the Bay of Marseille. Discharge volumes reached 4000 and 10,000 $m^3\ s^{-1}$ in the days preceding the intrusion events of June 2008 [*Pairaud et al*., 2011] and December 2003 [*Gatti et al*., 2006], respectively, which is rather high compared to the mean Rhone River discharge of around 1700 $m^3\ s^{-1}$.

By examining all the Rhone River discharge data before observed intrusion events in the Bay of Marseille between 2007 and 2011, we found that, contrary to our expectations, 50% of intrusion events occurred when the river discharge levels (maximum value during the 7 days preceding an intrusion) were smaller than the annual average of 1700 $m^3\ s^{-1}$. Moreover, there was a strong interannual variability in this result (Table 3). Thus, the occurrence of intrusion events appears to be decoupled from Rhone River discharge volumes.

While a high river discharge level did not appear to be a necessary prerequisite for intrusion events to occur, we tried to determine whether it was a sufficient one, i.e., whether the presence of above average discharge levels would inevitably induce an intrusion event. For our study period of 2007–2011, we counted 26 episodes during which we observed discharge levels in excess of 2500 $m^3\ s^{-1}$ that were sustained for a period of at least 1 day. However, only 31% of cases were followed by an intrusion event. In conclusion, high Rhone River discharge levels are neither necessary nor sufficient to induce intrusion events in the Bay of Marseille.

In order to further investigate the previous results which were based on observations, we performed a modeling experiment with two different simulations: one reference experiment (REF) with a realistic Rhone River

Table 3. Percentage of Intrusion Events Occurring During Times of High Rhone River Discharge Volumes (RRdis), a Shallow Thermocline Depth ($z_{th} < 40$ m), or During the Presence of the Marseille Eddy (ME)

Year	2007	2008	2009	2010	2011	2007–2011
RRdis (max of the 7 days before an intrusion) >1700 $m^3\ s^{-1}$	91	50	11	43	33	50
Thermocline depth < 40 m	64	88	78	86	100	79
Thermocline depth < 40m and/or RRdis > 1700 $m^3\ s^{-1}$	100	100	89	86	100	95
ME presence	78	100	100	86	100	90

discharge and a second experiment (R600) with a constant, low Rhone River discharge of 600 $m^3\ s^{-1}$. As the northern part of the Bay of Marseille is most affected by intrusion events (Figure A1), we chose to present the results of this analysis at the Northern Bay (NB) station (cf. Figure 1). Despite the considerably lower river discharge in the R600 experiment, we only observed a small reduction in the number of intrusion events during the year 2008 (Figure 3). Commensurate with our conclusions based on observations at the SOMLIT station (see above), the numerical results also confirmed that the Rhone River discharge volume was not an important driver for inducing intrusion events in the Bay of Marseille. However, most (77%) of the intrusion events which disappeared in the R600 experiment occurred between December and March (the nonstratified period). Thus, the Rhone River discharge appears to play a more important role in generating intrusions during the nonstratified winter months.

The duration of intrusion events observed in the R600 experiment was similar to the REF experiment. Nevertheless, intrusion events in the R600 experiment typically showed a smaller decrease in surface salinities compared to the reference run (Figure 3a).

3.2.2. Thermocline Depth

There is a strong degree of seasonality both in the vertical temperature profiles (Figure 4a) and in the occurrence of intrusion events (Table 2). By superimposing the occurrence of intrusion events on the seasonally varying thermocline depth Z_{th} (cf. equation (2)) (Figure 4b), we found that most intrusions (79%) occurred during the stratified period and in the presence of a relatively shallow thermocline depth above 40 m,

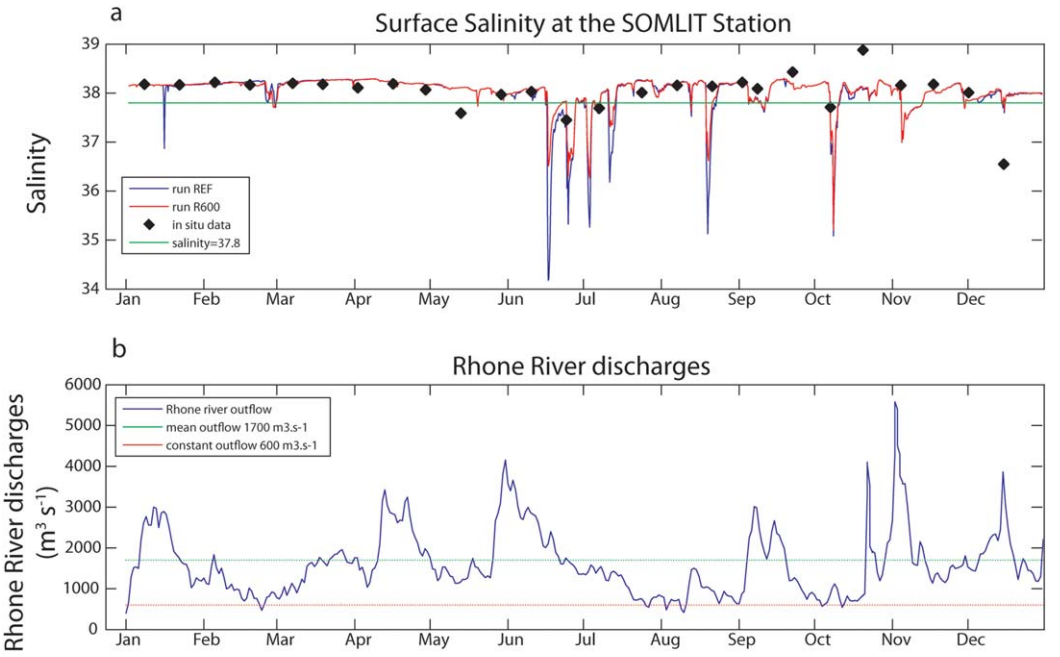

Figure 3. (a) Comparison of surface salinities between the run with realistic Rhone River discharges (run REF) and the run with constantly low Rhone River discharges (run R600) at the Northern Bay station (cf. Figure 1) for the year 2008. The green line represents the demarcation line for identifying an intrusion event, i.e., a salinity equal to 37.8; (b) comparing real Rhone River discharge volume (used in run REF) with the annual mean and the value of 600 $m^3\ s^{-1}$ chosen for the R600 run for the year 2008.

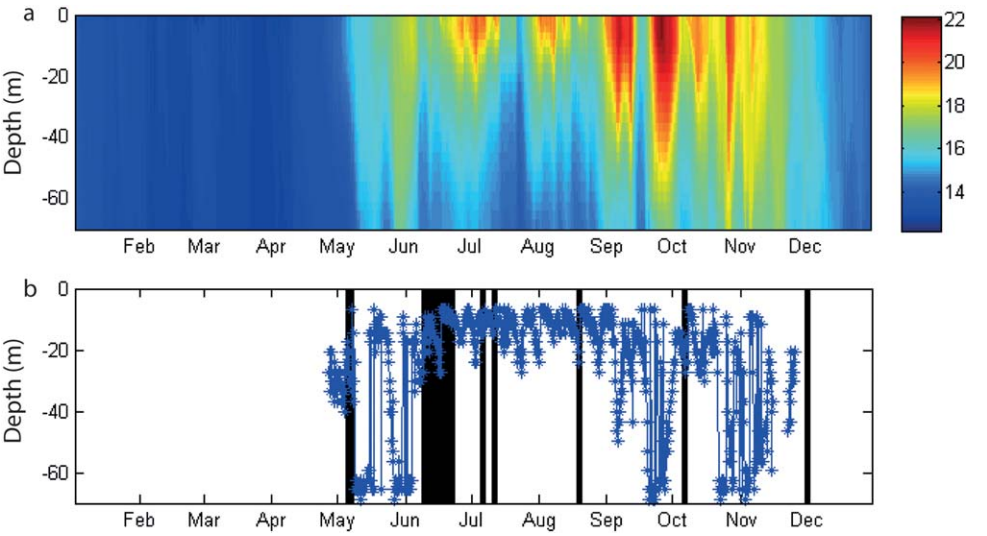

Figure 4. (a) Time series of modeled vertical temperature (in °C) at Northern Bay station for 2008. (b) Corresponding thermocline depth (Z_{th}) (blue line and stars) and intrusion events (black bars) at the Northern Bay station (cf. Figure 1) for the same period.

irrespective of the river discharge levels (Table 3). Typical thermocline depths which favored intrusions were between 7 and 20 m.

We found that 95% of intrusion events occurred during times when the water column was either stratified or with above average river discharge levels and only 5% (2 out of 38) were observed when the thermocline was deeper than 40 m and the river discharge levels below average (Figure 5).

3.2.3. Marseille Eddy (ME)

The ME is an anticyclonic eddy located between the Rhone River mouth and the Bay of Marseille [*Schaeffer et al.*, 2011]. Two different wind regimes have been shown to facilitate eddy generation: (i) a strong northerly offshore wind (Mistral) generates a vortex column due to the bathymetric constraint of a geostrophic barotropic current, which can surface after the wind relaxes; (ii) a southerly onshore wind generates a freshwater bulge from the Rhone River plume, which detaches from the coast and forms a well-defined anticyclonic surface eddy based on buoyancy gradients [*Schaeffer et al.*, 2011].

The ME eddy was also detected in the model simulations. In June 2008, the intrusion began on 17 June 2008 and a surface eddy had been present since 13 June 2008 down to about 30 m depth (Figures 6a–6c). In May 2011, the intrusion began on 19 May 2011 with the eddy present at 20 m depth since 11 May 2011 (Figures 6b–6d). Only during periods of weak winds, could the eddy characteristic velocity field be observed in the surface layer (e.g., on 17 June 2008, Figure 6b, and on 17 May 2011, Figure 6d).

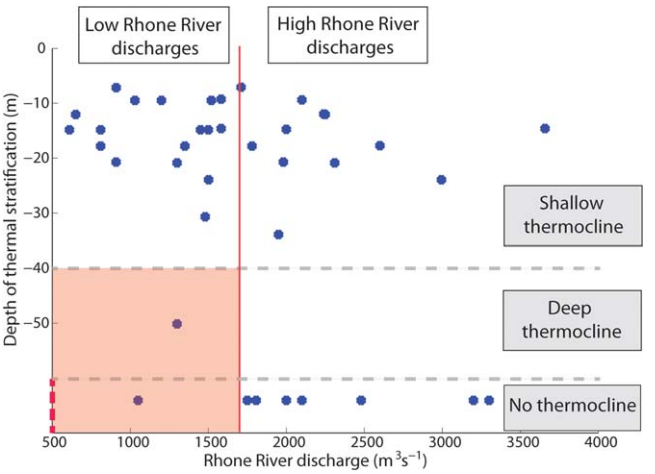

Figure 5. Occurrence of observed intrusion events as a function of Rhone River discharge level (RRdis) and thermocline depth for the years 2007–2011 at the Northern Bay Station (cf. Figure 1). Each dot represents one intrusion event.

Intrusion events were preceded by a ME in 90% of cases (Table 3). The anticyclonic eddy produces an eastward surface flow near the coast between the Rhone River mouth and the BoM. Plume water thus becomes trapped in the anticyclonic eddy and the eastward flow advects this low-salinity water toward the

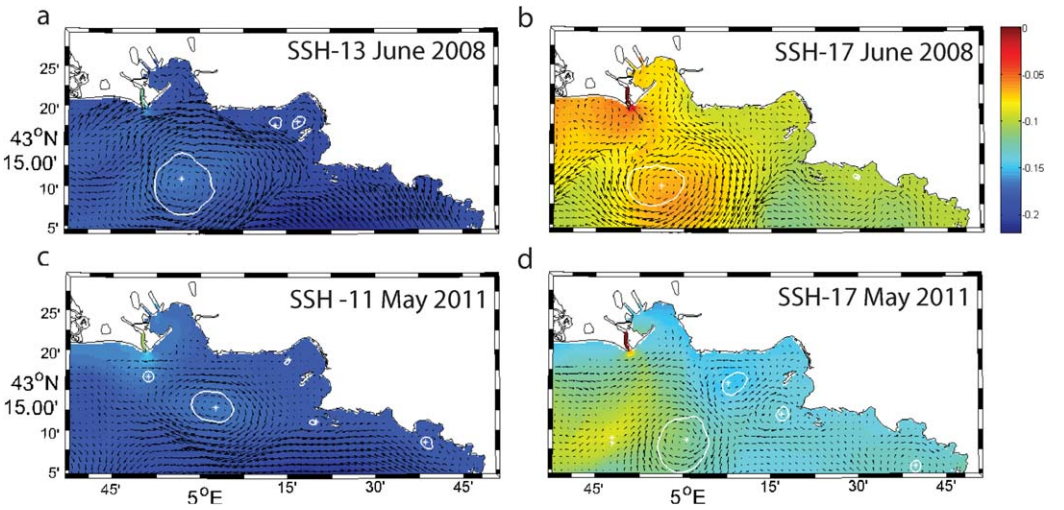

Figure 6. Eddy detection in fields of sea surface height (colors) and current velocity (arrows) at 20 m depth on (a) 13 June 2008 and (c) 11 May 2011 and at 2 m on (b) 17 June 2008 and (d) 17 May 2011.

Bay of Marseille. On 17 June 2008, the area located between the Rhone River mouth and the BoM was characterized by a high equivalent depth of freshwater (around 1 m, cf. Figure 2c) which corresponded to the location of the ME at that time.

However, the ME was detected numerous times in the model results and was not necessarily associated with or followed by an intrusion event. Consequently, the presence of the ME is necessary but not sufficient to induce an intrusion in the Bay of Marseille.

3.2.4. Wind

Due to the presence of strong and persistent winds in the Gulf of Lions (e.g., Mistral), the surface layer dynamics are strongly influenced by atmospheric forcing [*Schaeffer et al*., 2011]. For instance, wind forcing has been shown to be crucial for generating the ME [*Schaeffer et al*., 2011] (see section 3.2.3). Our analysis showed that wind forcing plays an important role before, during, and at the end of an intrusion event (Table 4).

3.2.4.1. Phase 1: Before an Intrusion Event

Intrusion events were often preceded by periods of weak winds (Table 4) which allowed the anticyclonic ME to extend to the surface layers thereby gaining contact and entrapping water from the Rhone River plume.

Despite the rarity of westerly winds in the Marseille coastal area, numerous intrusion events were preceded by winds from a westerly direction [cf. *Pairaud et al*., 2011, Figure 3]. Westerlies typically occur when the wind regime shifts between the dominant north-westerly and south-easterly directions. Indeed most of the intrusion events in our study were preceded by a shift in wind direction. This shift in wind direction seems to create favorable conditions to gradually push the Rhone River diluted water toward the Bay of Marseille.

Table 4. Observed Wind Regimes During the Different Phases of an Intrusion Event for the Years 2007–2011

	Wind Regime	Presence (in %)
Before an intrusion event (during the 5 days leading up to an event)	Regime shift between NW and SE directions	95
	Velocity < 1 m s^{-1}	81
	Velocity < 3 m s^{-1}	92
	Westerly	71
	North-westerly with velocities >3 m s^{-1}	89
	South-easterly with velocities >3 m s^{-1}	81
During an intrusion event	South-easterly	94
After an intrusion event	North-westerly with velocities >8 m s^{-1}	49
	South-easterly with velocities >8 m s^{-1}	20

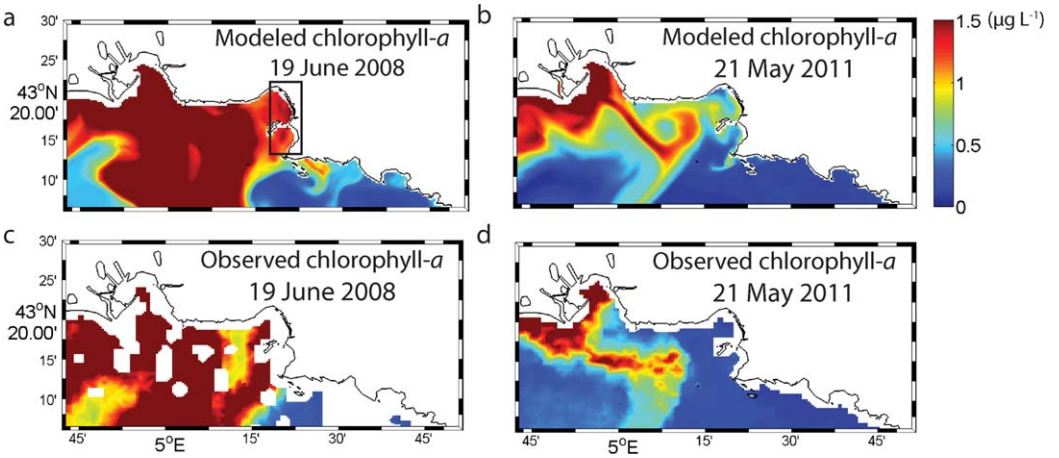

Figure 7. Comparison of modeled chlorophyll-*a* concentrations (in µmol L^{-1}) averaged over the top 10 m on (a) 19 June 2008, (b) 21 May 2011 with MODIS remote sensing images of ocean color on the same dates in plots (c) and (d). Remotely sensed chlorophyll-*a* concentrations are courtesy of Ifremer and were calculated using the OC5 algorithm [*Gohin et al.*, 2002].

3.2.4.2. Phase 2: During an Intrusion Event

South-easterly winds or generally weak winds were favorable to maintain Rhone River diluted water in the Bay of Marseille (Table 4).

3.2.4.3. Phase 3: Destruction of an Intrusion Event

The decline of an intrusion event was mainly driven by wind forcing. Strong winds lasting several hours or moderate winds lasting 1–2 days often led to the end of intrusion events by pushing the surface waters out of the Bay of Marseille.

3.3. Impact on the Ecosystem

We examined the biogeochemical impact of Rhone River intrusions on the ecosystem in the Bay of Marseille by analyzing surface maps of nutrients and chlorophyll-*a* and calculating mass balances for the different biogeochemical substances.

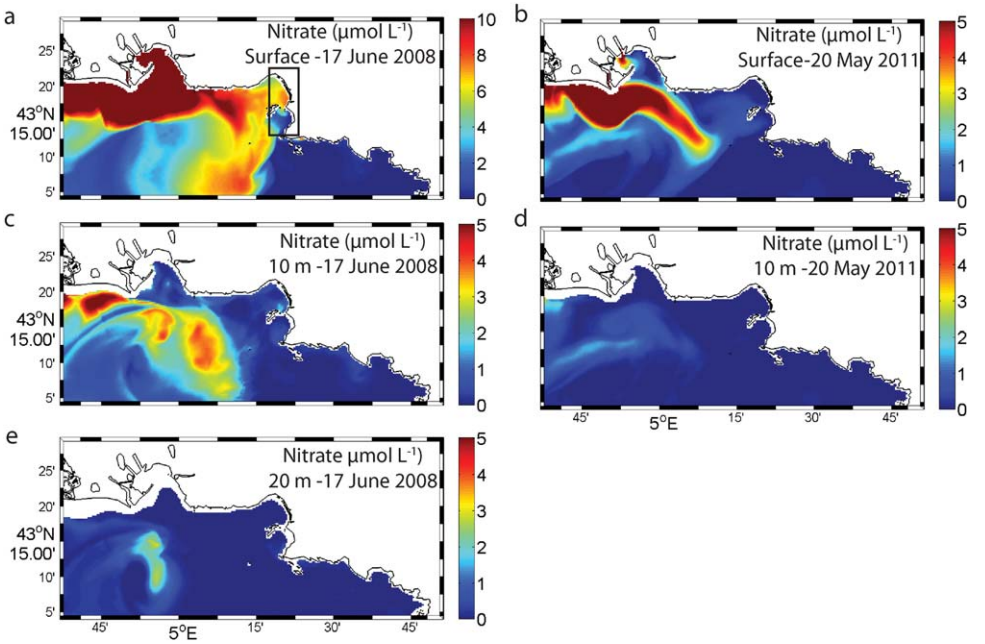

Figure 8. Modeled nitrate concentrations (µmol L^{-1}) on 17 June 2008 (a) at the surface (5 m average), (c) at 10 m (1 m average), (e) at 20 m (1 m average) and on 20 May 2011 (b) at the surface (5 m average) and (d) at 10 m (1 m average). The 20 m depth on 20 May 2011 is not shown as there is no visible trace of the plume.

3.3.1. Impact of Intrusion Events on Surface Nutrients and Chlorophyll-*a*

Following an intrusion event, the model results are in good agreement with remote sensing observations of ocean color on 19 June 2008 and 21 May 2011 (Figure 7) [see also *Fraysse et al*., 2013, Figure 7]. In both cases, the model is capable of reproducing both the spatial distribution and magnitude of chlorophyll-*a* concentrations which were present in the Rhone River diluted water (cf. Figure 2). The 5 year average chlorophyll-*a* concentration at the SOMLIT station is about 0.4 $\mu g\ L^{-1}$ for the period 2007–2011 [*Fraysse et al*., 2013]. During the intrusion events in June 2008 and May 2011, the chlorophyll-*a* concentration reached 1.5 and 0.8 $\mu g\ L^{-1}$, respectively (Figures 7a and 7b).

During the June 2008 intrusion, the simulated surface nitrate concentrations in the BoM were higher than during the May 2011 event, with values reaching 7 $\mu mol\ L^{-1}$ in the northern part while struggling to reach half this value in the southern part of the bay (Figure 8a). In comparison, surface nitrate concentrations hardly reached 3 $\mu mol\ L^{-1}$ during the small intrusion event in May 2011 (Figure 8b). Both in June 2008 and in May 2011, a tongue of high nitrate surface concentration extended from the Rhone River mouth toward the Bay of Marseille area. This tongue shape corresponds to the peripheral currents of the ME highlighted in Figure 6. The center of the ME remained at low nitrate concentrations at the surface.

While the surface nitrate concentrations were similar during both intrusion events, the situation at depth was very different. In June 2008, Rhone River diluted waters became trapped by the ME resulting in visibly elevated nitrate concentrations of 3 and 1.5 $\mu mol\ L^{-1}$ down to depths of 10 m (Figure 8c) and 20 m (Figure 8e), respectively. No elevated nitrate levels were present at depth during the May 2011 event (Figure 8d). The nutrient input and associated phytoplankton response therefore depends on the type of intrusion.

3.3.2. Quantification of the Biogeochemical Impact of RRIs on the Bay of Marseille

3.3.2.1. Intrusion of June 2008

As was outlined in section 2.2.3, we examined the biogeochemical impact of the Rhone River intrusions by comparing the mass budgets for a simulation with and without biogeochemical substances present in the Rhone River discharge. This allowed us to not only evaluate the amounts of nutrients input into the bay by an intrusion event but also the biological response of the local ecosystem (measured as an increase in total chlorophyll-*a*).

Based on the types of biogeochemical processes that occurred in the water column, the Rhone River intrusion of June 2008 can be divided into four distinct periods.

3.3.2.1.1. First Period: Beginning of the Intrusion, Inputs of Rhone River Diluted Water (16 June 2008)

At the beginning of the June 2008 intrusion, a large quantity of nitrogen of 1.9×10^9 mmol entered the bay, which would correspond to an increase in concentration of 0.6 $\mu mol\ L^{-1}$ if averaged over the entire bay. Most of the inorganic nitrogen was supplied as nitrate (1.6×10^9 mmol, blue curve in Figure 9a) and only negligible amounts as ammonium (Figure 9b). The allochthonous input of chlorophyll-*a* (Figure 9d) and carbon (Figure 9e) was less than 2×10^8 mg and 3.5×10^9 mmol, respectively.

3.3.2.1.2. Second Period: New Production (17–20 June 2008)

The consumption of nutrients led to new net production of chlorophyll-*a* of approximately 6×10^8 mg (green curve in Figure 9d) between 17 and 20 June 2008, which correspond to an average increase of 0.2 $\mu g\ L^{-1}$ of chlorophyll-*a* for the Bay of Marseille. However, the total stock of chlorophyll-*a* increased only by 4×10^8 mg (black curve) because the remaining 2×10^8 mg were exported (blue curve). This increase in chlorophyll-*a* is commensurate with an increase in the total carbon stock (Figure 9e). During this period, the increase and subsequent rapid decrease of nutrients (nitrate, phosphate) shows the advective input of nutrients and their rapid consumption by phytoplankton to sustain local new production (Figures 9a–9c). This coincided with an elevated local release of ammonium (green curve in Figure 9b) which led to an increase in the total ammonium stock (black curve). Advective contributions of ammonium were rather negligible and became negative once the bloom started to develop (blue curve in Figure 9b).

3.3.2.1.3. Third Period: Regenerated Production (20–24 June 2008)

In the days immediately following the intrusion event, there was very little net exchange of nutrients across the open boundaries and the stock of ammonium that was previously produced locally, decreased mostly because it was used to support the biological production inside the Bay of Marseille (Figure 9b).

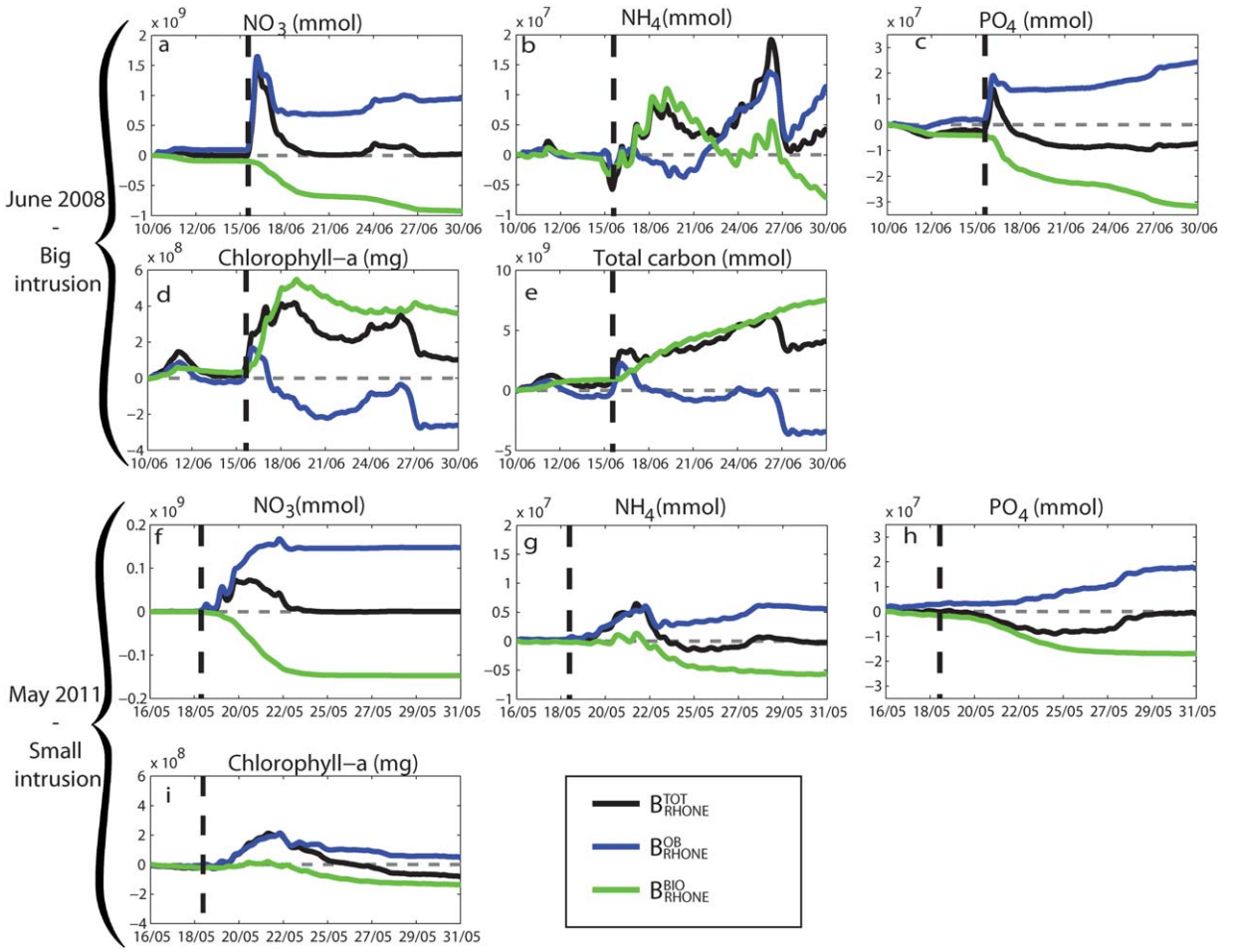

Figure 9. Mass balances of showing the impact of Rhone River intrusions (difference between runs "REF" and "NoRhone") in the Bay of Marseille box (cf. Figure 1) for different biogeochemical substances during the (big) June 2008 intrusion event from 10 June 2008 to 30 June 2008 for (a) nitrate, (b) ammonium, (c) phosphate, (d) chlorophyll-*a*, and (e) total carbon. (f–i) Corresponding plots for the (small) May 2011 intrusion event from 16 June 2011 to 31 May 2011. See Table 1 and section 2.2.3 for symbol definitions.

3.3.2.1.4. Fourth Period: Second Input of "Old" Rhone River Diluted Waters (24 June 2008)

The second input (24 June 2008) of Rhone River diluted water differed from the first one (16 June 2008) in that it was richer in ammonium (blue curve, Figure 9b) and chlorophyll-*a* (blue curve, Figure 9d) and poorer in nitrate (blue curve, Figure 9a) and phosphates (blue curve, Figure 9c). This second input thus shows characteristics of old Rhone River diluted waters where the new nutrients had already been consumed leading to elevated ammonium concentrations due to recycling via the microbial loop. The increase in chlorophyll-*a* during this period was mainly due to advective inputs, which is visible as a reduction in advective losses. This old Rhone River diluted water took a less direct path to the Bay of Marseille (possibly becoming trapped by the Marseille Eddy) which explains the different biogeochemical composition.

At the end of the intrusion, the total carbon stock in the bay due to Rhone River water input had increased by 6×10^9 mmol. The input of total carbon (2×10^9 mmol) at the beginning of the intrusion was balanced by the exports during the intrusion. The increase of the carbon in the bay was therefore due to local production (green curve in Figure 9e).

3.3.2.2. Intrusion of May 2011

The intrusion in May 2011 lasted only 3 days and the associated input of nitrate was about 10 times lower compared to June 2008 (Figure 9f versus Figure 9a, note the difference in scale). Contrary to June 2008, the total input of chlorophyll-*a* matched the increase in the standing stock almost exactly which suggests that local production was rather small. This lack of local production is further evidenced by the fact that the total increase in the stock of ammonium (black curve in Figure 9g) was solely due to advection (blue curve in Figure 9g). During the 2011 intrusion event (19–22 May 2011), there was no significant input of PO_4 (blue curve

Figure 9h) as the Rhone River diluted waters were already exhausted. This possible limitation of phytoplankton by phosphorus could explain why there was no local primary production associated with the May 2011 intrusion event (Figure 9i, green curve).

4. Discussion

In this study, we examined the occurrence of Rhone River water intrusions into the Bay of Marseille to the east of the Rhone River mouth. Such intrusions are rare (about 7 per year) but can have significant impacts on the local food web. We analyzed the frequency with which these intrusions occur, described possible generation mechanisms, and characterized their biogeochemical impact on the Bay of Marseille ecosystem.

4.1. Rhone River Intrusion Observation and Modeling

Typical intrusion events are difficult to observe both in situ and in silico because they occur at very short time scales, typically lasting less than 3 days. This may explain why there are only few references of such events in the literature [*Gatti et al*., 2006; *Para et al*., 2010]. From our observations, we estimated that Rhone River intrusions into the Bay of Marseille occurred on average 7.6 times per year, lasting an average total of 17 days per year (during our study period from 2007 to 2011). This is in good agreement with findings by *Gatti et al*. [2006] who found that intrusions were present at the SOFI station (cf. Figure 1) between 14 and 30 days per year. The slight discrepancy to their findings may be due to the fact that their SOFI site lies about 20 km southwest of our study area, which we chose to delimit at 5°17.3′E (western limit) and 43°13.05′N (southern limit). Due to the low temporal resolution of in situ data and the availability of satellite data of only around 30% and 40% of the time (see annex S5 in *Fraysse et al*. [2013]), this method likely underestimates the number of RRIs during the study period, as intrusions occurring during a period with no available in situ or remote sensing data were not counted.

Another reason why intrusions are difficult to observe in situ in the Bay of Marseille is that they typically occur in the northern part of the Bay (Figure A1), while the Somlit observational station is located in the southern part and therefore misses several (in particular of the smaller) intrusion events.

Initially, the model did not always reproduce the Rhone River intrusion events since several factors had to come together for an intrusion to occur. Only once all these factors were well represented by the model did the model adequately reproduce an event, both in terms of duration and spatial extent. One case in point is wind. A good representation of wind forcing (direction, intensity with adequate spatial and temporal resolution) is crucial to model the hydrodynamics in coastal seas and in particular for modeling Rhone River intrusions. Intrusions lasting only 1 or 2 days (e.g., in May 2011) were more difficult to reproduce with the model than the long intrusions (such as the one in June 2008).

4.2. Assumptions on the Generation Processes and Classification of Rhone River Intrusions

We suggested that four different factors could be involved in facilitating the generation of Rhone River intrusion events in the Bay of Marseille: the Rhone River discharge volume, the presence and depth of a thermocline, the anticyclonic Marseille Eddy, and the dominant wind direction and intensity. While none of these factors on their own appeared capable of inducing Rhone River intrusions, certain combinations of some or all of these factors always seemed to lead to an intrusion event. Only two of the four factors mentioned above were found to be necessary (albeit not sufficient) for an intrusion to occur. They are: (i) the presence of the Marseille Eddy and (ii) favorable wind conditions. Vertical temperature stratification is not necessary if the Rhone River discharge levels are high. On the other hand, if discharge levels are low, intrusions only occur if the water column has a shallow thermocline allowing the plume water to glide far enough south to make contact with the eddy (Figure 10).

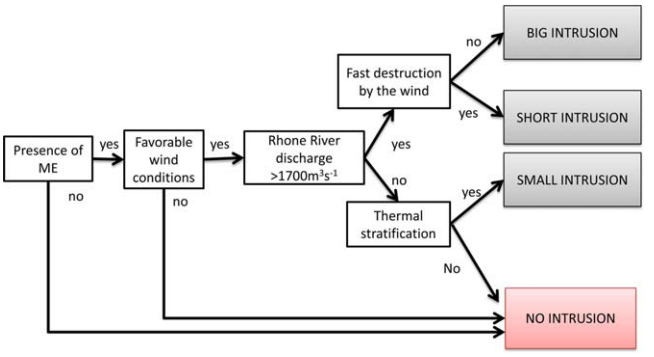

Figure 10. Logical flowchart to explain the different generation processes for the different types of Rhone River intrusions.

Based on the size and duration of an intrusion, we can distinguish between three different kinds which also have slightly different generation processes (Figure 10):

1. "Big" intrusions are induced by the presence of the ME, favorable winds, Rhone River discharges higher than 1700 $m^3 s^{-1}$, and a late destruction (winds remaining favorable for a sufficiently long time). The intrusion of June 2008 is an example of such a "big" intrusion.
2. "Short-lived" intrusions exhibit the same characteristics as "big" intrusions (presence of the ME, favorable winds, Rhone River discharges higher than 1700 $m^3 s^{-1}$), except that wind conditions do not remain favorable for a sufficiently long time to produce a "big" event.
3. "Small" intrusions are induced by the presence of the ME, favorable winds, Rhone River discharges lower than 1700 $m^3 s^{-1}$, and a shallow thermocline. In this case, the shallow thermocline is necessary to allow the plume water to flow far enough south in order to make contact with ME. The intrusion occurring in May 2011 is an example of such a "small" event.

During the years from 2007 to 2011, the proportion of intrusions falling into each of the three categories "big," "short-lived," and "small," are 8%, 39%, and 53%, respectively.

We can thus establish various scenarios that can lead to the generation of an intrusion event. Under standard NW wind conditions, the Rhone River plume extends in a SW direction (Figure 11a). The Rhone River discharge volume and the presence and depth of a thermocline are important in order to bring Rhone River water into contact with the northern edge of the ME where the anticyclonic flow pushes the plume water eastward to the Bay of Marseille. This contact is brought about either by a sufficiently high discharge volume (Figure 11d) (irrespective of stratification) or—in case of low discharge volumes—the presence of a strong and shallow thermocline (Figure 11b) which allows Rhone River diluted waters to flow far enough south in order to get in contact with the eddy.

In situations where the Rhone River discharge volume is weak, a shallow thermocline allows plume water to come into contact with the ME which then advects this water toward the BoM with SE winds pushing it onshore (Figure 11b). These SE winds may cause this small tongue of plume water to become disconnected from the eddy and be pushed into the BoM (Figure 11c). Since plume water only comes into contact with the northern edge of the eddy, only small quantities of plume water are advected toward the Bay of Marseille, leading to a "small" intrusion event.

In situations where the discharge volume is high, the extent of the plume is sufficiently large and some of it becomes trapped in the ME (Figure 11e). If this occurs and the wind changes from NW to a SE direction, the trapped plume water gets pushed into the BoM leading to a "big" or "short-lived" intrusion event (depending on the persistence of favorable wind conditions) (Figure 11f). When the winds become unfavorable, the intrusion is destroyed either by NW winds pushing the plume waters offshore (Figure 11g) or by persisting SE winds leading to a downwelling of plume water near the coast (Figure 11f). The impact on the Bay of Marseille is identical for both destruction mechanisms: Rhone River waters were exported out of the Bay leading to a significant export of biogeochemical substance offshore. Finally, the main difference between "big" and "small" intrusions is the quantity of water transported into the Bay of Marseille. Due to their different generation mechanisms, "big" intrusions impact down to a depth of 20 m while "small" instructions only affect the surface.

4.3. Comparison With Previous Work

Gatti et al. [2006] proposed three hypotheses to explain the generation process of Rhone River water intrusions in the Bay of Marseille. Although their work predates more recent studies confirming the existence of the Marseille Eddy [*Allou et al.*, 2010] and the associated eddy generation process [*Schaeffer et al.*, 2011], *Gatti et al.* [2006] already speculated about the possible existence of an anticyclonic eddy which produces an eastward displacement of plume water in two of their three hypotheses. Our model results confirm this hypothesis (Figure 10).

Gatti et al. [2006] also reported that on 17–19 June 1998, a barotropic eastward current [*Petrenko*, 2003] carrying diluted coastal water ($S < 37.7$ at 20 m depth) [*Diaz*, 2000] had been detected at the SOFI site after an 8 day Mistral event. The fact that the intrusion occurred at the end of a period of sustained

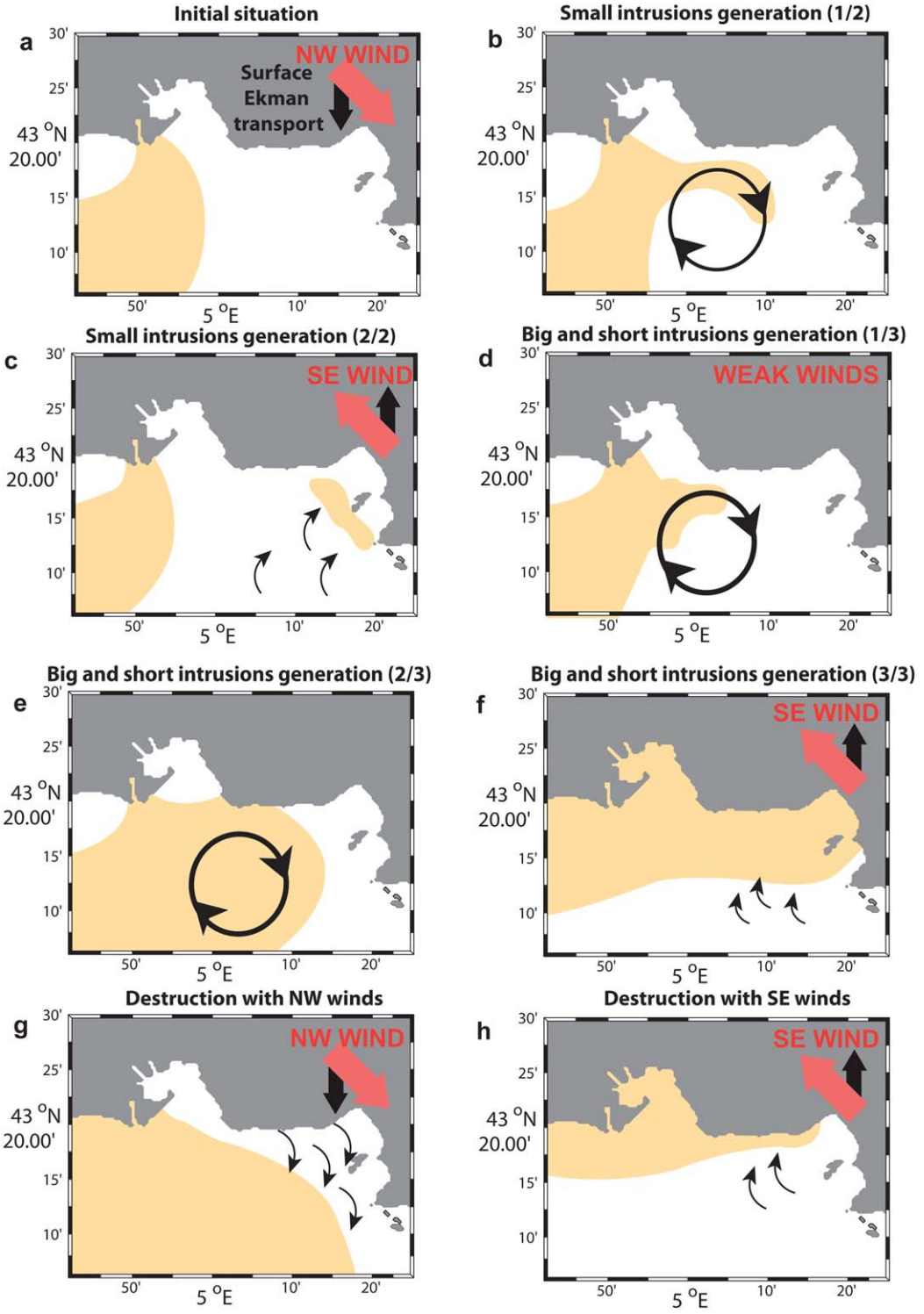

Figure 11. Graphical representation of (a) a typical situation with the westward displacement of the Rhone River plume and the different generation mechanisms leading to (b and c) a small and (d and f) a big/short-lived intrusion. (g and h) Two different destruction mechanisms.

strong north-westerly winds agrees with the ME generation process proposed by *Schaeffer et al.* [2011]. The date of the intrusion (17–19 June 1998) suggests that the water column was stratified and the depth of the intrusion (20 m) would correspond to the thermocline depth. Thus, our summary scheme (Figure 10) and scenarios (Figure 11) seem to be in agreement with some of the scenarios previously suggested by others.

A number of studies have shown that wind stress is an important forcing agent for river plume dynamics in the coastal zone [*Choi and Wilkin*, 2007; *Marques et al*., 2009; *Xia et al*., 2010]. In the Pacific Northwest coast, a recent plume study highlighted that a sequence of wind could be important to bring water to the coast [*Giddings et al*., 2014]. It was demonstrated that the intermittency in the wind forcing may be important to drive coastal transport which appeared to be higher during years with more frequent relaxation/downwelling events. These results may also be relevant to our study area as the number of intrusions per year could be related to the wind intermittency. Our results strongly suggest that the shift between mistral and southeasterly wind regimes is a necessary requirement to generate an intrusion event.

4.4. Impact of Rhone River Intrusions on the Bay of Marseille Ecosystem

The impact of Rhone River intrusions on the coastal ecosystem of the Bay of Marseille was highly dependent upon (i) the time of year in which the intrusion occurred and (ii) the type of intrusion (small, short-lived, or big).

Most intrusions occur between May and October, a time of year when the water column is either depleted or at least limited in nutrients [*Fraysse et al*., 2013]. During this period, the nutrients brought by Rhone River intrusions are rapidly consumed, fueling local biological production. In contrast, intrusions occurring in winter should not have any significant impact on the primary production because nutrients are typically not limiting due to the strong vertical winter mixing which leads to light but not nutrient limitation [*Fraysse et al*., 2013]. It is therefore not relevant that the nitrate concentration in the Rhone River discharge is typically lower in summer compared to winter (60 versus 170 μmol L^{-1}). The same seasonal signal is also present in the phosphate concentrations although less pronounced.

Other factors influencing the magnitude of the impact of intrusions on the Bay of Marseille ecosystem are (1) the age of the plume water reaching the bay, (2) the duration of an event, and (3) the spatial extent (or type) of the intrusion. Small intrusions only advect small quantities of plume water into the bay which are often quickly exported again, leaving little time for biogeochemical processes to transfer these inputs to higher trophic levels. So the overall biogeochemical impact of "small" intrusions tends to be low.

"Short-lived" and "big" intrusion events occur when the Rhone River discharge volume is high. The sheer quantity of nutrients delivered to the Bay of Marseille means that their impact on the ecosystem is larger and longer lived.

Due to their different generation mechanisms, the nutrient cocktail delivered to the bay may vary for different types of intrusions. Small intrusions only brush the northern edge of the ME before being advected to the Bay of Marseille. Hence they carry a relatively small volume of plume water that can already be nutrient limited or depleted. This water is typically richer in ammonium but may be limited in phosphate and nitrate due to local production having occurred during the transit, which in turn leads to allochthonous inputs of chlorophyll-*a* into the bay (e.g., during the May 2011 intrusion). For big and short-lived intrusions, on the other hand, the sheer volume of plume water entering the Bay is much larger, which leads to autochthonous inputs of chlorophyll-*a* into the bay (e.g., during the June 2008 intrusion). This result is supported by a study on fluorescence and absorption properties of chromophoric dissolved organic matter (CDOM) at the SOMLIT station. *Para et al*. [2010] observed that in June 2008 the Rhone River plume reached the Bay of Marseille and induced a local phytoplankton blooms and subsequent fluorescent chromophoric dissolved organic matter (CDOM) production without adding terrestrial fluorescence signatures. The increase of primary production during intrusion events and the associated storage of carbon by the primary producers represent a sink of CO_2 as the carbon fixed by phytoplankton is quickly transferred to higher trophic levels and exported out of the bay. When the intrusion was not destroyed by strong winds (case of a "big" intrusion), the maturation of Rhone River inputs continued due to biogeochemical processes. Because the inputs of organic matter and other nutrients fueled the microbial loop, a recycling of the nutrients occurred, spurring regenerated production.

The strong impact of large plumes on coastal ecosystems have also been demonstrated in other regions such as Indonesia and US Pacific northwest region [*Jennerjahn et al*., 2004; *Hickey et al*., 2010]. In the Adriatic Sea, the influence of the Po River discharge on phytoplankton dynamics has been shown to extend as far as 100 km from the Po River leading to a significant increase in local production and intense algal blooms [*Penna et al*., 2004].

Overall, our study confirms the pivotal role that the ME plays for the generation of intrusion events, and the dispersion or retention of biogeochemical material at local scales [cf. *Schaeffer et al*., 2011].

5. Conclusion

This study highlighted that Rhone River intrusions can be of great ecological significance for the Bay of Marseille ecosystem. For our study period (2007–2011), intrusion events occurred on average 7.6 times per year and were more frequently observed during summer and in the northern part of the bay.

Intrusion events appeared to be induced by a complex interplay of factors that include: (i) wind forcing, (ii) the presence of an anticyclonic eddy (the "Marseille Eddy"), (iii) the variability in Rhone River discharge volume, and (iv) the variability in thermocline depth and strength. While each of the above factors appeared to be important for generating an intrusion, neither of them on their own would be sufficient to create such an event. Winds appear to be a crucial factor for triggering an intrusion and allowing for it to persist. In summary we found that:

1. High Rhone River discharge volumes or the presence of a shallow thermocline are necessary to permit the Rhone River plume to spread over a sufficiently large area.
2. Eastward surface flows associated with the anticyclonic Marseille Eddy are necessary to advect the Rhone River diluted waters toward the Bay of Marseille.
3. Favorable wind conditions (winds turning at the right moment from NW to SE, weak winds during the intrusion event, etc.) were required to induce the south-eastward flow of the low salinity surface water and maintain an intrusion once it had occurred.

Based on the duration and spatial extent of an intrusion, they can be placed into one of the following three categories: (i) short-lived, (ii) big, and (iii) small. Each category has a different impact on the local biogeochemistry and thus the ecosystem in the Bay of Marseille. Only the "short-lived" and "big" intrusions are capable of giving a significant boost to new primary production and stimulating the microbial loop. "Small" intrusions lead to a much smaller increase in production. However, through the allochthonous input of phytoplankton cells, "small" intrusions can still provide a stimulus to secondary producers.

These different ecological impacts are tightly linked to the respective generation processes for each type of intrusion. While the ME was always necessary in the generation processes, it played a different role for each type of intrusion. To generate a "big" intrusion, plume water became entrapped by the Marseille Eddy (ME), which allowed it to preserve its plume characteristics for a longer time and also caused the nitracline to deepen. For "small" intrusions, on the other hand, the plume water only brushes the northern edge of the ME which still allows water to be transported eastward but in much smaller quantities. Thus, big intrusions bring larger quantities of material and impact deeper in the water column, while "small" intrusions impact only the surface.

Most (53%) of the intrusions observed from 2007 to 2011 were "small." Nevertheless, the less frequent "big" (8%) and "short-lived" (39%) intrusions have the greatest biogeochemical impact on the Bay of Marseille as they provide a valuable stimulus to local production in an otherwise oligotrophic ecosystem.

Appendix A: Self-Organizing Map (SOM)

Self-Organizing Maps (SOMs) have become one of the standard analysis tools in oceanographic research [*Richardson et al*., 2003; *Liu and Weisberg*, 2011; *Allen et al*., 2007; *Liu et al*., 2007] and more specifically in river plume characterization [*Liu et al*., 2009; *Falcieri et al*., 2014]. SOMs have been shown to be more powerful for feature extraction than some of the more conventional methods such as Empirical Orthogonal Functions [*Liu and Weisberg*, 2011; *Liu et al*., 2006]. They represent a kind of unsupervised Artificial Neural Network that is well suited for the analysis of multivariate data sets because they provide a topology-preserving nonlinear projection of the data set in a regular two-dimensional space, called a "map," and therefore constitute a methodology for nonlinear ordination analysis [*Kohonen*, 2001; *Solidoro et al*., 2007].

The SOM analysis was performed using SOM_PAK Version 3.1 which is produced by and freely available from the Neural Network Research Centre at the Helsinki University of Technology (http://www.cis.hut.fi/~hynde/lvq/).

In this study, we used SOMs to analyze the frequency of synoptic salinity patterns and to identify their seasonal cycle. We used the approach described by *Richardson et al.* [2003] in which they analyzed the frequency

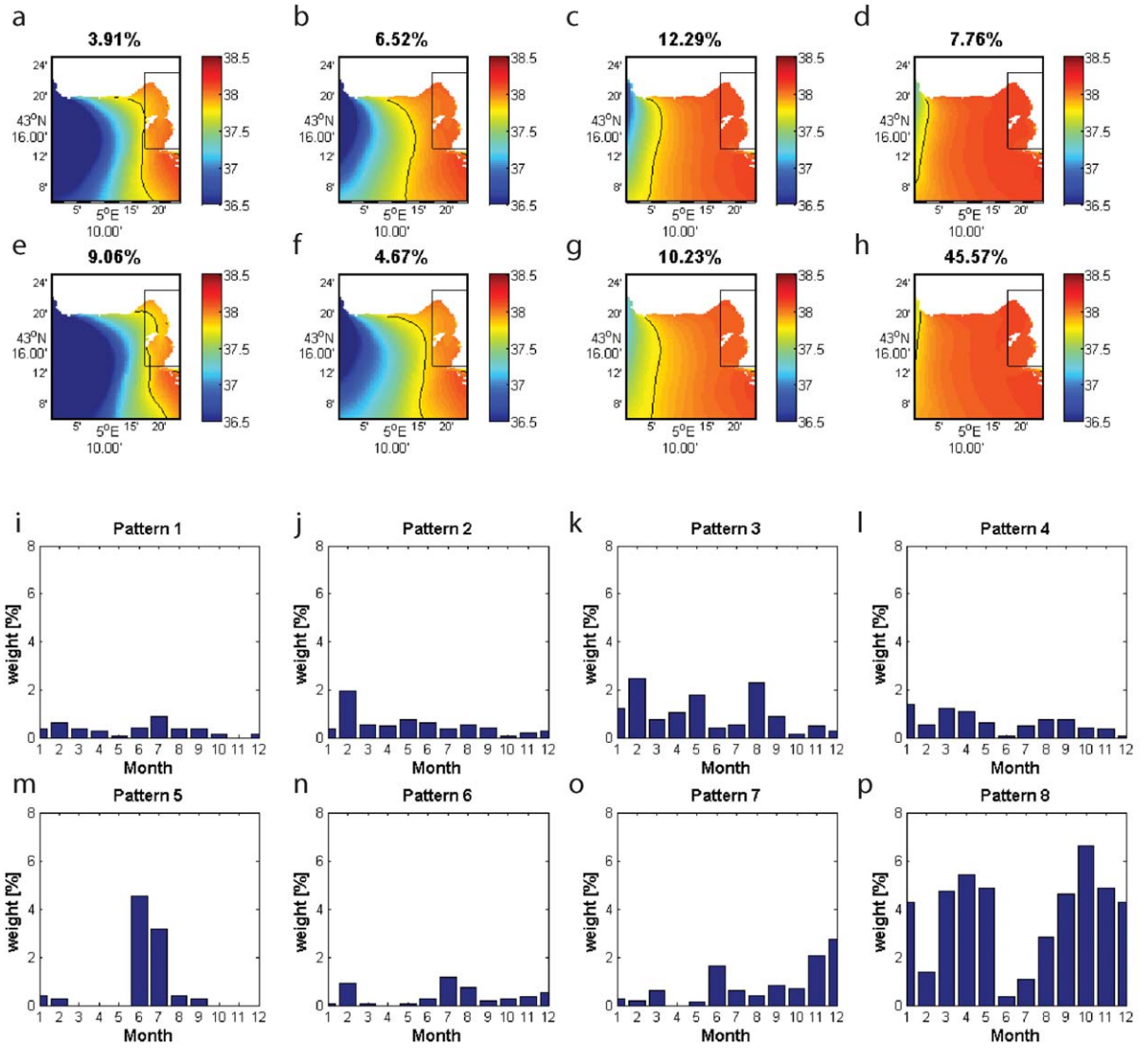

Figure A1. (a–h) The 2 × 4 patterns of a self-organizing map of surface salinities for the Bay of Marseille. The frequency of occurrence is given above each map. The black rectangle shows the boundaries of the Bay of Marseille. The isohaline of 37.8 is represented by the thin black line. (i–p) Monthly distribution of the frequency of occurrence for each pattern.

and seasonal cycle of synoptic sea surface temperature (SST) [see *Richardson et al*., 2003, Figures 8 and 9]. In practice, when using a SOM, one has to decide a priori the size of the map, i.e., the number and arrangement in two-dimensional space of the neurons (the neural network) and a few parameters of the training algorithm (training length, neighborhood function, and learning rate), but no further assumptions on the database structure are needed.

The characteristics of the SOM are summarized in Table A1. The choice of the number of neurons is to some extent subjective. If too few neurons are chosen, important features may not be resolved, while too many may render the results too complex and difficult to interpret [*Allen et al*., 2007]. After extensive testing we chose a 4 × 2 array. However, the general conclusions of this study are not sensitive to the choice of map size. Most of the other tunable SOM parameters were chosen according to the practical method given by *Liu et al*. [2006] for small map sizes. A notable exception is the neighborhood function which was Gaussian.

A1. Frequency and Seasonality of Rhone River Intrusion Events Studied With SOMs

Self-organizing maps were used to analyze the frequency of occurrence of eight different synoptic salinity patterns for the year 2008 (Figures A1a–A1h). Typical salinities in the Bay of Marseille range from 38 to 38.5

Table A1. Characteristics of the Self-Organizing Map

Structure of neural network	Lattice of the network	Rectangular
	Shape of the network	Sheet
	Size of the network	4×2 array
Learning algorithm	Initialization process	Linear
	Training length	Long
	Learning process	Batch
	Neighborhood function	Gaussian

and were present about 91% of the time in 2008 (Figures A1a–A1d and A1f–A1h). Only during 9% of the time, the pattern matched with the definition of a Rhone River intrusion showing salinities of less than 37.8 in the Bay of Marseille (Figure A1e). In addition, the typical salinity pattern during an intrusion suggests that intrusion events mostly affect the northern part of the bay.

The monthly distribution of each pattern (Figures A1i–A1p) confirmed the results presented in Table 2 that intrusion events exhibited a clear seasonal variability and were more likely to occur during the early summer months of June and July (Figure A1m).

Appendix B: Mass Budgets Details

The total matter (M^{TOT}, in mmol) at time t can be obtained by integrating the concentration (C, in mmol m^{-3}) of a biogeochemical substance (BS) over the volume of the Bay of Marseille box:

$$M^{TOT}(BS,t)=\iiint_V C(BS,t)dV \tag{B1}$$

The budget B^{TOT} (in mmol) corresponds to the cumulative change in total matter within the box relative to the initial stock at t_0:

$$B^{TOT}(BS,t)=M^{TOT}(BS,t)-M^{TOT}(BS,t_0)\equiv\Delta M^{TOT}(BS) \tag{B2}$$

The budget B^{ATM} (in mmol) corresponds to the cumulative quantity of matter deposited from the atmosphere between t_0 and t at the sea surface (S) of the box. If F^{ATM} denotes the flux (in mmol s^{-1} m^2) through the sea surface of the box we can calculate the budget from:

$$B^{ATM}(BS,t)=\int_{t_0}^{t}\oiint_S F^{ATM}dSdt \tag{B3}$$

The budget B^{UR} (in mmol) corresponds to the cumulative quantity of matter input by the urban rivers between t_0 and t. Assuming that Q denote the total water flow of all urban rivers (in m^3 s^{-1}) and C^{RIV}(BS,t) the concentration of the biogeochemical substance BS in these rivers (in mmol m^{-3}) then input by urban rivers can be quantified as:

$$B^{UR}(BS,t)=\int_{t_0}^{t}Q(t)C^{UR}(BS,t)dt \tag{B4}$$

The budget B^{OB} (in mmol) corresponds to the cumulative quantity of matter exchanged across the open boundaries of the box between t_0 and t due to advective/diffusive processes. If F^{OB} denotes the total mass flux across the open boundaries (in mmol s^{-1}) at time t, then changes in BS due to in/outflows at the boundaries can be calculated from:

$$B^{OB}(BS,t)=\int_{t_0}^{t}F^{OB}(BS,t)dt \tag{B5}$$

If $F^{OB}(BS,t) > 0$ (<0) there is a net influx (outflux) of the biogeochemical substance (BS) and the slope of B^{OB} would be positive (negative).

The budget B^{BIO} (in mmol) accounts for the cumulative amount of matter produced or consumed by the biogeochemical processes inside the box between times t_0 and t. If we define $Tend^{BIO}$ (in mmol s^{-1}) as the

amount of the biogeochemical substance (BS) produced or consumed per unit of time, we obtain the evolution of the biogeochemical substance BS from:

$$B^{BIO}(BS,t)=\int_{t_0}^{t} Tend^{BIO}(BS,t)dt \quad \text{(B6)}$$

If $Tend^{BIO}(BS,t) > 0$ (<0) there is a net production (consumption) of the biogeochemical substance (BS) at time t and the slope of B^{BIO} is positive (negative).

Acknowledgments

The authors acknowledge the staff of the Somlit National Network for Coastal Observations (INSU-CNRS) for providing the data time series, the Compagnie Nationale du Rhone for the data on Rhone River discharges and Meteo France. The authors thanks the GFSC, Greenbelt, MD 20771, for the production and distribution of MODIS ocean color data, and ESA for the production and distribution of MERIS ocean color data, processed by the Ifremer algorithms in Brest. The Rhone concentration data were provided by the National MOOSE Program (Mediterranean Oceanic Observing System on Environment) and the Service d'Observation of the Mediterranean Institute of Oceanography (MIO). The authors gratefully acknowledge P. Raimbault, N. Garcia, V. Lagadec, and M. Fornier for analytical and field assistance. This work was supported by the PACA region, IFREMER grant, GIRAC, and PNEC-EC2CO MASSILIA projects, sustained by the water agency (AERMC). This study was also part of the "Mistrals MERMEX (WP3-C3A)" project sustained by the international "IMBER" project and the European PERSEUS project (EC grant agreement 287600). ONR wishes to acknowledge financial support from the AMICO-BIO project (12-MCGOT-GMES-1-CVS-047). The authors also thank Francesco Nencioli for his eddy tracking package, Benedicte Thouvenin for her help on the Mars3D model, Martin Huret for providing scripts, Christophe Yohia and Maurice Libes for the cluster maintenance, and Anne Petrenko and Andrea Doglioli for fruitful discussions. We thank the two anonymous reviewers for their helpful comments to improve this paper.

References

Allen, J. I., P. J. Somerfield, and F. J. Gilbert (2007), Quantifying uncertainty in high-resolution coupled hydrodynamic-ecosystem models, *J. Mar. Syst.*, *64*(1-4), 3–14, doi:10.1016/j.jmarsys.2006.02.010.

Allou, A., P. Forget, and J.-L. Devenon (2010), Submesoscale vortex structures at the entrance of the Gulf of Lions in the Northwestern Mediterranean Sea, *Cont. Shelf Res.*, *30*(7), 724–732, doi:10.1016/j.csr.2010.01.006.

Arnoux-Chiavassa, S., V. Rey, and P. Fraunié (2003), Modeling 3D Rhône river plume using a higher order advection scheme, *Oceanol. Acta*, *26*(4), 299–309, doi:10.1016/S0399-1784(03)00058-6.

Auger, P. A., F. Diaz, C. Ulses, C. Estournel, J. Neveux, F. Joux, M. Pujo-Pay, and J. J. Naudin (2011), Functioning of the planktonic ecosystem on the Gulf of Lions shelf (NW Mediterranean) during spring and its impact on the carbon deposition: A field data and 3-D modelling combined approach, *Biogeosciences*, *8*(11), 3231–3261, doi:10.5194/bg-8-3231-2011.

Baklouti, M., F. Diaz, C. Pinazo, V. Faure, and B. Quéguiner (2006), Investigation of mechanistic formulations depicting phytoplankton dynamics for models of marine pelagic ecosystems and description of a new model, *Prog. Oceanogr.*, *71*(1), 1–33, doi:10.1016/j.pocean.2006.05.002.

Broche, P., J.-L. Devenon, P. Forget, J.-C. de Maistre, J.-J. Naudin, and G. Cauwet (1998), Experimental study of the Rhone plume. Part I: Physics and dynamics, *Oceanol. Acta*, *21*(6), 725–738, doi:10.1016/S0399-1784(99)80002-4.

Choi, B.-J., and J. L. Wilkin (2007), The effect of wind on the dispersal of the Hudson River Plume, *J. Phys. Oceanogr.*, *37*(7), 1878–1897, doi:10.1175/JPO3081.1.

Craig, R. K., and J. B. Ruhl (2010), Governing for sustainable coasts: Complexity, climate change, and coastal ecosystem protection, *Sustainability*, *2*(5), 1361–1388, doi:10.3390/su2051361.

Demarcq, H., and L. Wald (1984), La dynamique superficielle du panache du Rhône d' après l ' imagerie infrarouge satellitaire, *Oceanol. Acta*, *7*(2), 159–162.

Diaz, F. (2000), Evolution saisonnière de la production primaire et des processus d'assimilation–régénération de l'azote dans le Golfe du Lion. Estimation d'un bilan de carbone. Approches in situ et modélisation (tome I), PhD thesis, 270 pp., Univ. Aix-Marseille 2, Marseille, France.

Diaz, F., J.-J. Naudin, C. Courties, P. Rimmelin, and L. Oriol (2008), Biogeochemical and ecological functioning of the low-salinity water lenses in the region of the Rhone River freshwater influence, NW Mediterranean Sea, *Cont. Shelf Res.*, *28*(12), 1511–1526, doi:10.1016/j.csr.2007.08.009.

Durrieu de Madron, X., et al. (2011), Marine ecosystems' responses to climatic and anthropogenic forcings in the Mediterranean, *Prog. Oceanogr.*, *91*(2), 97–166, doi:10.1016/j.pocean.2011.02.003.

Elliott, M. (2011), Marine science and management means tackling exogenic unmanaged pressures and endogenic managed pressures—A numbered guide, *Mar. Pollut. Bull.*, *62*(4), 651–655, doi:10.1016/j.marpolbul.2010.11.033.

Estournel, C., P. Broche, P. Marsaleix, J. L. Devenon, F. Auclair, and R. Vehil (2001), The Rhone River plume in unsteady conditions: numerical and experimental results, *Estuarine Coastal Shelf Sci.*, *53*, 25–38.

Falcieri, F. M., A. Benetazzo, M. Sclavo, A. Russo, and S. Carniel (2014), Po River plume pattern variability investigated from model data, *Cont. Shelf Res.*, doi:10.1016/j.csr.2013.11.001, in press.

Faure, V., C. Pinazo, J.-P. Torréton, and P. Douillet (2006), Relevance of various formulations of phytoplankton chlorophyll a: Carbon ratio in a 3D marine ecosystem model, *C. R. Biol.*, *329*(10), 813–822, doi:10.1016/j.crvi.2006.07.006.

Faure, V., C. Pinazo, J.-P. Torreton, and S. Jacquet (2010), Modelling the spatial and temporal variability of the SW lagoon of New Caledonia I: A new biogeochemical model based on microbial loop recycling, *Mar. Pollut. Bull.*, *61*(7-12), 465–479, doi:10.1016/j.marpolbul.2010.06.041.

Forget, P., and S. Ouillon (1998), Surface suspended matter off the Rhone river mouth from visible satellite imagery, *Oceanol. Acta*, *21*(6), 739–749.

Fraysse, M., C. Pinazo, V. Faure, P. Raimbault, P. Lazzari, and I. L. Pairaud (2013), Development of a 3D coupled physical-biogeochemical model for the Marseille coastal area (NW Mediterranean Sea): What complexity is required in the coastal zone?, *PLoS ONE*, *8*(12), e80012, doi:10.1371/journal.pone.0080012.

Gatti, J., A. Petrenko, J.-L. Devenon, Y. Leredde, and C. Ulses (2006), The Rhone river dilution zone present in the northeastern shelf of the Gulf of Lion in December 2003, *Cont. Shelf Res.*, *26*(15), 1794–1805, doi:10.1016/j.csr.2006.05.012.

Giddings, S. N., P. MacCready, B. M. Hickey, N. S. Banas, K. A. Davis, S. A. Siedlecki, V. L. Trainer, R. M. Kudela, N. A. Pelland, and T. P. Connolly (2014), Hindcasts of potential harmful algal bloom transport pathways on the Pacific Northwest coast, *J. Geophys. Res. Oceans*, *119*, 2439–2461, doi:10.1002/2013JC009622.

Gohin, F., J. N. Druon, and L. Lampert (2002), A five channel chlorophyll concentration algorithm applied to SeaWiFS data processed by SeaDAS in coastal waters, *Int. J. Remote Sens.*, *23*(8), 1639–1661, doi:10.1080/01431160110071879.

Gohin, F., S. Loyer, M. Lunven, C. Labry, J.-M. Froidefond, D. Delmas, M. Huret, and A. Herbland (2005), Satellite-derived parameters for biological modelling in coastal waters: Illustration over the eastern continental shelf of the Bay of Biscay, *Remote Sens. Environ.*, *95*(1), 29–46, doi:10.1016/j.rse.2004.11.007.

Hickey, B. M., et al. (2010), River influences on shelf ecosystems: Introduction and synthesis, *J. Geophys. Res.*, *115*, C00B17, doi:10.1029/2009JC005452.

Huret, M., M. Sourisseau, P. Petitgas, C. Struski, F. Léger, and P. Lazure (2012), A multi-decadal hindcast of a physical–biogeochemical model and derived oceanographic indices in the Bay of Biscay, *J. Mar. Syst.*, *109–110*, S77–S94, doi:10.1016/j.jmarsys.2012.02.009.

Ibanez, C., D. Pont, and N. Prat (1997), Characterization of the Ebre and Rhone estuaries: A basis for defining and classifying salt-wedge estuaries, *Limnol. Oceanogr.*, *42*(1), 89–101.

Jany, C., I. Pairaud, B. Thouvenin, and R. Verney (2012), METROC: Modélisation idéalisée de substances dissoutes et particulaires rejetées en rade de Marseille, IFREMER internal report # RST. ODE/LER/PAC/12-21, 56 pp., Ifremer, Brest, France.

Jennerjahn, T., V. Ittekkot, S. Klöpper, S. Adi, S. P. Nugroho, N. Sudiana, A. Yusmal, and B. Gaye-Haake (2004), Biogeochemistry of a tropical river affected by human activities in its catchment: Brantas River estuary and coastal waters of Madura Strait, Java, Indonesia, *Estuarine Coastal Shelf Sci.*, *60*(3), 503–514, doi:10.1016/j.ecss.2004.02.008.

Kohonen, T. (2001), *Self-Organizing Maps*, 3rd ed., Springer, Berlin, Heidelberg.

Lazure, P., and F. Dumas (2008), An external–internal mode coupling for a 3D hydrodynamical model for applications at regional scale (MARS), *Adv. Water Resour.*, *31*(2), 233–250, doi:10.1016/j.advwatres.2007.06.010.

Liu, Y., and R. H. Weisberg (2011), A review of self-organizing map applications in meteorology and oceanography, in *Self-Organizing Maps: Applications and Novel Algorithm Design*, edited by J. I. Mwasiagi, pp. 253–272, InTech, Rijeka, Croatia, doi:10.5772/13146.

Liu, Y., R. H. Weisberg, and C. N. K. Mooers (2006), Performance evaluation of the self-organizing map for feature extraction, *J. Geophys. Res.*, *111*, C05018, doi:10.1029/2005JC003117.

Liu, Y., R. H. Weisberg, and L. K. Shay (2007), Current patterns on the West Florida shelf from joint self-organizing map analyses of HF radar and ADCP data, *J. Atmos. Oceanic Technol.*, *24*(4), 702–712, doi:10.1175/JTECH1999.1.

Liu, Y., P. MacCready, and B. M. Hickey (2009), Columbia River plume patterns in summer 2004 as revealed by a hindcast coastal ocean circulation model, *Geophys. Res. Lett.*, *36*, L02601, doi:10.1029/2008GL036447.

Ludwig, W., E. Dumont, M. Meybeck, and S. Heussner (2009), River discharges of water and nutrients to the Mediterranean and Black Sea: Major drivers for ecosystem changes during past and future decades?, *Prog. Oceanogr.*, *80*(3-4), 199–217, doi:10.1016/j.pocean.2009.02.001.

Marques, W. C., E. H. Fernandes, I. O. Monteiro, and O. O. Möller (2009), Numerical modeling of the Patos Lagoon coastal plume, Brazil, *Cont. Shelf Res.*, *29*(3), 556–571, doi:10.1016/j.csr.2008.09.022.

Naudin, J.-J., G. Cauwet, C. Fajon, L. Oriol, S. Terzić, J.-L. Devenon, and P. Broche (2001), Effect of mixing on microbial communities in the Rhone River plume, *J. Mar. Syst.*, *28*(3-4), 203–227, doi:10.1016/S0924-7963(01)00004-5.

Nencioli, F., C. Dong, T. Dickey, L. Washburn, and J. C. McWilliams (2010), A vector geometry–based eddy detection algorithm and its application to a high-resolution numerical model product and high-frequency radar surface velocities in the Southern California bight, *J. Atmos. Oceanic Technol.*, *27*(3), 564–579, doi:10.1175/2009JTECHO725.1.

Oursel, B., C. Garnier, I. Pairaud, D. Omanović, G. Durrieu, A. D. Syakti, C. Le Poupon, B. Thouvenin, and Y. Lucas (2014), Behaviour and fate of urban particles in coastal waters: Settling rate, size distribution and metals contamination characterization, *Estuarine Coastal Shelf Sci.*, *138*, 14–26, doi:10.1016/j.ecss.2013.12.002.

Pairaud, I. L., J. Gatti, N. Bensoussan, R. Verney, and P. Garreau (2011), Hydrology and circulation in a coastal area off Marseille: Validation of a nested 3D model with observations, *J. Mar. Syst.*, *88*(1), 20–33, doi:10.1016/j.jmarsys.2011.02.010.

Para, J., P. G. Coble, B. Charrière, M. Tedetti, C. Fontana, and R. Sempéré (2010), Fluorescence and absorption properties of chromophoric dissolved organic matter (CDOM) in coastal surface waters of the northwestern Mediterranean Sea, influence of the Rhône River, *Biogeosciences*, *7*(12), 4083–4103, doi:10.5194/bg-7-4083-2010.

Penna, N., S. Capellacci, and F. Ricci (2004), The influence of the Po River discharge on phytoplankton bloom dynamics along the coastline of Pesaro (Italy) in the Adriatic Sea., *Mar. Pollut. Bull.*, *48*(3–4), 321–326, doi:10.1016/j.marpolbul.2003.08.007.

Petrenko, A. (2003), Variability of circulation features in the Gulf of Lion NW Mediterranean Sea. Importance of inertial currents, *Oceanol. Acta*, *26*(4), 323–338, doi:10.1016/S0399-1784(03)00038-0.

Pont, D., J.-P. Simonnet, and A. V. Walter (2002), Medium-term changes in suspended sediment delivery to the ocean: Consequences of catchment heterogeneity and river management (Rhône River, France), *Estuarine Coastal Shelf Sci.*, *54*(1), 1–18, doi:10.1006/ecss.2001.0829.

Pujo-Pay, M., P. Conan, F. Joux, L. Oriol, J. Naudin, and G. Cauwet (2006), Impact of phytoplankton and bacterial production on nutrient and DOM uptake in the Rhône River plume (NW Mediterranean), *Mar. Ecol. Prog. Ser.*, *315*(3), 43–54, doi:10.3354/meps315043.

Reffray, G., P. Fraunie, and P. Marsaleix (2004), Secondary flows induced by wind forcing in the Rhone region of freshwater influence, *Ocean Dyn.*, *54*(2), 179–196, doi:10.1007/s10236-003-0079-y.

Richardson, A. J., C. Risien, and F. Shillington (2003), Using self-organizing maps to identify patterns in satellite imagery, *Prog. Oceanogr.*, *59*(2-3), 223–239, doi:10.1016/j.pocean.2003.07.006.

Schaeffer, A., A. Molcard, P. Forget, P. Fraunié, and P. Garreau (2011), Generation mechanisms for mesoscale eddies in the Gulf of Lions: Radar observation and modeling, *Ocean Dyn.*, *61*(10), 1587–1609.

Solidoro, C., V. Bandelj, P. Barbieri, G. Cossarini, and S. Fonda Umani (2007), Understanding dynamic of biogeochemical properties in the northern Adriatic Sea by using self-organizing maps and k-means clustering, *J. Geophys. Res.*, *112*, C07S90, doi:10.1029/2006JC003553.

Xia, M., L. Xie, and L. J. Pietrafesa (2010), Winds and the orientation of a coastal plane estuary plume, *Geophys. Res. Lett.*, *37*, L19601, doi:10.1029/2010GL044494.

Younes, W., N. Bensoussan, J.-C. Romano, D. Arlhac, and M.-G. Lafont (2003), Seasonal and interannual variations (1996–2000) of the coastal waters east of the Rhone River mouth as indicated by the SORCOM series, *Oceanol. Acta*, *26*(4), 311–321, doi:10.1016/S0399-1784(03)00037-9.